MOX–Report No. 14/2007

Reduced Basis Method for Parametrized Advection-Reaction Problems

Luca Dedé

MOX, Dipartimento di Matematica "F. Brioschi"
Politecnico di Milano, Via Bonardi 29 - 20133 Milano (Italy)

mox@mate.polimi.it http://mox.polimi.it

Reduced Basis Method for Parametrized Advection–Reaction Problems*

Luca DEDE'

3^{rd} September 2007

MOX – Modeling & Scientific Computing
Dipartimento di Matematica
Politecnico di Milano
via Bonardi 9, I–20133, Milano, Italy
luca.dede@polimi.it

Abstract

In this work we consider the Reduced Basis method for the solution of parametrized advection–reaction partial differential equations. For the generation of the basis we adopt a stabilized Finite Element method and we define the Reduced Basis method in the "primal–dual" formulation for this stabilized problem. We provide both a priori and a posteriori Reduced Basis error estimates and we discuss the effects of the Finite Element approximation on the Reduced Basis error. We propose an adaptive algorithm for the selection of the sample sets upon which the basis are built. The basic idea of this algorithm is the minimization of the computational costs associated with the solution of the Reduced Basis problem. Numerical tests shows the convenience, in terms of computational costs, of the "primal–dual" Reduced Basis approach.

Keywords: *Parametrized advection–reaction Partial Differential Equations; Reduced Basis method; "primal–dual" Reduced Basis approach; stabilized Finite Element method; a posteriori error estimation; computational costs saving.*

Introduction

The Reduced Basis (RB) method is a computational approach which allows rapid and reliable predictions of functional outputs of Partial Differential Equations (PDEs) with parametric dependence [6, 11, 12, 13, 14]. Indeed, the RB method has a wide range of relevant applications in the characterization of engineering components or systems which require the prediction of certain "quantities of interest" or performance metrics: e.g., deflections, maximum stresses, maximum temperatures, heat transfer rates, flow rates, aerodynamical forces or momentum. This method has already been applied to the cases of Stokes and Navier–Stokes equations [10, 16, 22, 23, 27], as well as to linear elasticity problems [11, 26] and many other physical applications (see e.g. [2, 5, 14]). Environmental problems represent a promising field of application for the RB method. Preliminary investigations have been considered in [15, 17] for pollution problems in

*This work has been partially supported by "Progetto Roberto Rocca", M.I.T.–Politecnico di Milano collaboration.

air, for which the RB method has been adopted to evaluate the concentration of pollutants emitted by industrial sites in certain zones of observation, such as cities [4]. Parametrized steady advection–diffusion PDEs have been adopted in order to describe such phenomena. In particular, both geometrical and physical parameters have been considered, such as the location of industrial plants, the intensity or direction of the wind field, or the diffusion coefficient.

This work deals with the investigation of the RB method for the evaluation of outputs, which depend on the solution of parametrized advection–reaction PDEs; this in view of Environmental applications, for which the diffusion phenomena are negligible w.r.t. the trasport and reaction ones. The solution of such PDEs stands for the concentration of a pollutant in a medium, such as air or water, in a $2D$ domain.

The RB method is based on the decoupling of the generation and the projection stages of the approximation procedures, which leads to a decoupled offline–online computational approach. The complexity of the offline step, in which the basis are generated, depends on the dimension of the "truth" space, say N_t, to which belongs the "truth" solution corresponding to a given value of the parameters vector. The complexity of the online stage depends on the dimension of the RB space, say N, with $N \ll N_t$, and the complexity of the parametric dependence.
For the definition of the "truth" space, we make use of the Finite Element (FE) method [19]. In order to get rid of the instabilities caused by the transport term of the hyperbolic advection–reaction PDE, we use the Streamline Diffusion Finite Element (SDFE) stabilized method [19, 28]. This leads to the transformation of the original hyperbolic PDE into a new one, with elliptic nature. We define the RB method for this parametrized stabilized advection–reaction problem, for which the affine decomposition property holds. Moreover, we consider the "primal–dual" RB approach [11, 13, 24], which requires the definition of a dual problem. This approach is well–suited both for the approximation and the error evaluation of the output and, as we highlight in this work, also for the reduction of the computational costs associated with the RB online stage w.r.t. those of the "only primal" RB approach (without the dual problem). We provide a priori RB error estimates for both the solution and the output, thus evidencing the role of the FE approximation and stabilization in the RB method. In fact, the total error on the solution or the output is composed by two parts corresponding to the FE and RB approximations, respectively. In particular, we show that the "complexity" of the RB increases, as the FE approximation improves by reducing the mesh size (i.e. the parametrized stabilized problem tends to assume an hyperbolic nature). We also provide the a posteriori RB error estimate for the output according to [13, 24]. We remark that the idea of using stabilized FE for the definition of the "truth" space has been already introduced in [15], even if a priori and a posteriori RB estimates, as well as an error analysis for the FE and RB approximations, have not been provided. Then, we propose a general adaptive algorithm for the choice of the sample sets (used for the definition of the RB basis), for which the a posteriori RB estimate is used. We base our adaptive algorithm on a criterium of minimization of the online computational costs.
Two numerical tests, inspired by Environmental problems, are provided dealing with both physical and geometrical parametrizations. Moreover, we experimentally show that the RB approximation is stable, if the FE one is stable.

This paper is organized as follows. In Section 1 we introduce the parametrized advection–reaction PDEs in an abstract setting. We consider two specific problems (regarded as Problem 1 and Problem 2) with physical and geometrical parameters. A particular case of Problem 1, say Problem 1(bis), is also introduced. In Section 2 we provide the FE

approximation of the parametrized problem, after having introduced the stabilization by means of the SDFE method. An a priori error analysis for the Problem 1(bis) is reported; some estimates and other mathematical tools, which we use in the following Sections, are introduced as well. Section 3 deals with the RB method, which is described for the particular problem in consideration; the "primal–dual" RB approach is considered for the solution of the RB problem. Both a priori and a posteriori RB estimates are provided. Moreover, the adaptive algorithm for the choice of the samples sets is outlined. In Section 4 we report some considerations about the numerical solution of the parametrized advection–reaction PDEs, by using jointly the FE and the RB methods. We provide in Section 5 two numerical tests referring to Problems 1 and 2 of Section 1. Concluding remarks follow.

1 Parametrized Advection–Reaction Equations

In this Section we introduce in an abstract setting the parametrized advection–reaction PDEs and, in view of the numerical tests of Section 4, we specify two particular problems with physical and geometrical parameters.

1.1 An abstract parametrized problem

Let us indicate with $\boldsymbol{\mu}$ the vector of parameters s.t. $\boldsymbol{\mu} := (\mu_1, \ldots, \mu_P) \in \mathcal{D}$, being $\mathcal{D} \subset \mathbb{R}^P$, with $P \in \mathbb{N}$ the domain of parameters. We consider the following advection–reaction PDE:

$$\begin{cases} \mathbf{b}(\boldsymbol{\mu}) \cdot \nabla \phi + \sigma(\boldsymbol{\mu})\phi = f(\boldsymbol{\mu}) & \text{in } \Omega, \\ \phi = 0 & \text{on } \Gamma_D, \end{cases} \tag{1}$$

where $\Omega \subset \mathbb{R}^2$ is a bi–dimensional domain with boundary $\partial\Omega$. The parametrized advection field $\mathbf{b}(\boldsymbol{\mu}) \in [L^\infty(\Omega)]^2 \ \forall \boldsymbol{\mu} \in \mathcal{D}$ is chosen s.t. $\nabla \cdot \mathbf{b}(\boldsymbol{\mu}) = 0 \ \forall \boldsymbol{\mu} \in \mathcal{D}$, the parametrized reaction term $\sigma(\boldsymbol{\mu}) \in L^\infty(\Omega) \ \forall \boldsymbol{\mu} \in \mathcal{D}$, s.t. $\sigma(\boldsymbol{\mu}) > 0 \ \forall \boldsymbol{\mu} \in \mathcal{D}$, and the parametrized source term $f(\boldsymbol{\mu}) \in L^2(\Omega) \ \forall \boldsymbol{\mu} \in \mathcal{D}$. For the sake of simplicity, we have omitted to explicitly express the dependence of $\mathbf{b}(\boldsymbol{\mu})$, $\sigma(\boldsymbol{\mu})$ and $f(\boldsymbol{\mu})$ on the spatial coordinate $\mathbf{x} \in \mathbb{R}^2$, which should be read as $\mathbf{b}(\boldsymbol{\mu}, \mathbf{x})$, $\sigma(\boldsymbol{\mu}, \mathbf{x})$ and $f(\boldsymbol{\mu}, \mathbf{x})$ respectively. We also observe that not all the functions $\mathbf{b}$, σ and f must necessarily depend on the set of parameters. Moreover, we suppose that the parametrized data admit the *affine decomposition* property, e.g.: $\mathbf{b}(\boldsymbol{\mu}) = \mathbf{b}(\boldsymbol{\mu}, \mathbf{x}) = \left(\sum_{i=1}^{M_{b1}} \Theta_i^{b1}(\boldsymbol{\mu}) g_i^{b1}(\mathbf{x}), \sum_{j=1}^{M_{b2}} \Theta_j^{b2}(\boldsymbol{\mu}) g_j^{b2}(\mathbf{x}) \right)$, with $\Theta_i^{b1}(\boldsymbol{\mu})$, $\Theta_j^{b2}(\boldsymbol{\mu}) \in C^1(\mathcal{D})$, $g_i^{b1}(\mathbf{x})$, $g_j^{b2}(\mathbf{x}) \in L^\infty(\Omega)$, $i = 1, \ldots, M_{b1}$, $j = 1, \ldots, M_{b2}$, for some M_{b1}, $M_{b2} \in \mathbb{N}$. In the same manner the reaction term reads: $\sigma(\boldsymbol{\mu}) = \sigma(\boldsymbol{\mu}, \mathbf{x}) = \sum_{i=1}^{M_\sigma} \Theta_i^\sigma(\boldsymbol{\mu}) g_i^\sigma(\mathbf{x})$, with $\Theta_j^\sigma(\boldsymbol{\mu}) \in C^1(\mathcal{D})$ and $g_i^\sigma(\mathbf{x}) \in L^\infty(\Omega)$, $i = 1, \ldots, M_\sigma$, for some $M_\sigma \in \mathbb{N}$; finally, the source term is: $f(\boldsymbol{\mu}) = f(\boldsymbol{\mu}, \mathbf{x}) = \sum_{i=1}^{M_f} \Theta_i^f(\boldsymbol{\mu}) g_i^f(\mathbf{x})$, with $\Theta_j^f(\boldsymbol{\mu}) \in C^1(\mathcal{D})$ and $g_i^f(\mathbf{x}) \in L^2(\Omega)$, $i = 1, \ldots, M_f$, for some $M_f \in \mathbb{N}$. We define the part of the boundary $\partial\Omega$ indicated with Γ_D as $\Gamma_D(\boldsymbol{\mu}) := \{\mathbf{x} \in \partial\Omega \ : \ \mathbf{b}(\boldsymbol{\mu}) \cdot \hat{\mathbf{n}} < 0 \ \forall \boldsymbol{\mu} \in \mathcal{D}\}$ which corresponds to the inflow boundary, being $\hat{\mathbf{n}}$ the outward directed unit vector normal to $\partial\Omega$. Moreover, we assume that the boundary $\Gamma_D(\boldsymbol{\mu})$ is "fixed", in the sense that $\Gamma_D(\boldsymbol{\mu}) = \Gamma_D \ \forall \boldsymbol{\mu} \in \mathcal{D}$; finally, we define Γ_N as $\Gamma_N := \partial\Omega \backslash \Gamma_D$, i.e. the outflow boundary.
The weak form of problem (1) reads:

$$\text{find} \ \ \phi(\boldsymbol{\mu}) \in \mathcal{V} \ \ : \ \ A(\phi(\boldsymbol{\mu}), v; \boldsymbol{\mu}) = F(v; \boldsymbol{\mu}) \qquad \forall v \in \mathcal{V}, \ \ \forall \boldsymbol{\mu} \in \mathcal{D}, \tag{2}$$

where $\mathcal{V} := H^1_{\Gamma_D}(\Omega)$, being $H^1_{\Gamma_D}(\Omega)$ the usual Hilbert space of functions with null trace on Γ_D (see e.g. [9]), and:

$$A(w, v; \boldsymbol{\mu}) := \int_\Omega \left(\mathbf{b}(\boldsymbol{\mu}) \cdot \nabla w \, v + \sigma(\boldsymbol{\mu}) \, w \, v\right) \, d\Omega, \qquad F(v; \boldsymbol{\mu}) := \int_\Omega f(\boldsymbol{\mu}) \, v \, d\Omega. \tag{3}$$

Due to the affine decomposition assumptions made for the data $\mathbf{b}(\boldsymbol{\mu})$, $\sigma(\boldsymbol{\mu})$ and $f(\boldsymbol{\mu})$, the bilinear form $A(\cdot, \cdot; \boldsymbol{\mu})$ and the functional $F(\cdot; \boldsymbol{\mu})$ can be re–written as:

$$A(w, v; \boldsymbol{\mu}) = \sum_{q=1}^{Q} \vartheta_q(\boldsymbol{\mu}) A_q(w, v), \qquad F(v; \boldsymbol{\mu}) = \sum_{q=1}^{Q^F} \vartheta_q^F(\boldsymbol{\mu}) F_q(v). \tag{4}$$

for some $Q \in \mathbb{N}$ and $Q^F \in \mathbb{N}$ with the bilinear forms $A_q(\cdot, \cdot)$ and the linear functionals $F_q(\cdot)$ not depending on $\boldsymbol{\mu}$.
Our goal consists in calculating an output $s(\boldsymbol{\mu})$ depending on the parameter $\boldsymbol{\mu}$:

$$s(\boldsymbol{\mu}) = L\left(\phi(\boldsymbol{\mu}); \boldsymbol{\mu}\right) \qquad \forall \boldsymbol{\mu} \in \mathcal{D}, \tag{5}$$

where $L(\cdot; \boldsymbol{\mu})$ is a linear and continuous functional acting from $\mathcal{V}$ to $\mathbb{R}$, s.t.:

$$L(v; \boldsymbol{\mu}) := \int_\Omega \gamma(\boldsymbol{\mu}) \, v \, d\Omega, \tag{6}$$

being $\gamma(\boldsymbol{\mu})$ a parameter function for which the same hypothesis of affine decomposition made for $f(\boldsymbol{\mu})$ holds, s.t.:

$$s(\boldsymbol{\mu}) = \sum_{q=1}^{Q^L} \vartheta_q^L(\boldsymbol{\mu}) L_q\left(\phi(\boldsymbol{\mu})\right), \tag{7}$$

for some $Q^L \in \mathbb{N}$ and the linear functionals $L_q(\cdot)$ independent on $\boldsymbol{\mu}$.

1.2 Problem 1: physical parametrization

In this Section we consider a particular case, say "Problem 1", of the general advection–reaction problem described in Section 1.1, with a physical parameter.
We set $\boldsymbol{\mu} = \mu$, with μ a physical parameter which can be regarded as the magnitude of an advection field, whose direction is given by the unit vector $\mathbf{V} \in \mathbb{R}^2$. By referring to the abstract problem (1) we chose $\mathbf{b}(\mu) = \mu \mathbf{V}$, $\sigma(\mu) = 1$ and $f(\mu) = g$ (independent on μ); moreover, we assume $\mathcal{D} = [\mu_{min}, \mu_{max}] \subset \mathbb{R}$ and $\gamma(\mu) = \delta$ (independent on μ). The corresponding advection–reaction problem reads:

$$\begin{cases} \mu \mathbf{V} \cdot \nabla \phi + \phi = g & \text{in } \Omega, \\ \phi = 0 & \text{on } \Gamma_D, \end{cases} \tag{8}$$

for which the generic weak form (2) follows. In this case we have $Q = 2$, $Q^F = 1$ and $Q^L = 1$, with $F(v; \mu)$ and $L(v; \mu)$ both independent on μ.

1.3 Problem 2: physical and geometrical parametrization

We consider now a parametrized problem with both geometrical and physical parameters; this allows as to vary the shape of domain by acting on the values of the geometrical parameter (see [16, 20, 21, 22, 23]). We will refer to this problem as "Problem 2".
Let us introduce a geometrical parameter μ_g, s.t. $\boldsymbol{\mu} = (\mu_p, \mu_g) \in \mathcal{D} \subset \mathbb{R}^2$, where μ_p is the physical parameter introduced in Section 1.2. We remark that the domain depends now on μ_g; from a computational point of view this could lead to a relevant computational effort in terms of time–work. In order to overcome this difficulty, we map the real domain into a reference domain, which is "fixed" as the geometrical parameter vary, and we transform the original problem into a new one set on the reference domain. By indicating with the subscript 0 the quantities defined on the real domain $\Omega_0 = \Omega_0(\mu_g)$, the parametrized advection–reaction PDE reads:

$$\begin{cases} \mu_p \mathbf{V}_0 \cdot \nabla_0 \phi_0 + \phi_0 = g_0 & \text{in } \Omega_0(\mu_g), \\ \phi_0 = 0 & \text{on } \Gamma_{0D}(\mu_g), \end{cases} \tag{9}$$

with the same notation of Section 1.2. The problem on Ω_0 in weak form would read:

$$\text{find} \quad \phi_0(\boldsymbol{\mu}) \in \mathcal{V}_0 \quad : \quad A_0(\phi_0(\boldsymbol{\mu}), v; \boldsymbol{\mu}) = F_0(v; \boldsymbol{\mu}) \qquad \forall v \in \mathcal{V}_0, \quad \forall \boldsymbol{\mu} \in \mathcal{D}, \tag{10}$$

where $\mathcal{V}_0 := H^1_{\Gamma_{0D}}(\Omega_0(\mu_g))$; moreover, $s(\boldsymbol{\mu}) = \int_{\Omega_0(\mu_g)} \delta_0 \, v \, d\Omega_0(\mu_g)$. Let us suppose that an *affine map*, acting from a reference domain Ω to the real domain $\Omega_0(\mu_g)$, could be provided and expressed in the following form:

$$\mathbf{x}_0 = T(\mu_g)\mathbf{x} + \mathbf{t}(\mu_g), \tag{11}$$

being the tensor $T(\mu_g) \in \mathbb{R}^{2\times 2}$ and the vector $\mathbf{t}(\mu_g) \in \mathbb{R}^2$. In the case that the domains Ω_0 and Ω are partitioned into subdomains Ω_{0i}, Ω_i, s.t. $\cup_i \Omega_{0i} = \Omega_0$ and $\cup_i \Omega_i = \Omega$, it is necessary to define an affine map for each subdomain; however, for the sake of simplicity, we consider only the case of non partitioned domains, even if it is a straightforward matter to generalize to the case with subdomains.
By using the affine map, the weak problem (8) can be re–written in weak form as in Eq.(2), where $\mathcal{V} := H^1_{\Gamma_D}(\Omega)$ and $A(\cdot, \cdot; \boldsymbol{\mu})$, $F(\cdot; \boldsymbol{\mu})$ are defined in Eq.(3) and set on the reference domain Ω. By referring to the general problem of Section 1.1 and by inspection of the weak form (2), it is possible to deduce the data:

$$\begin{aligned} \mathbf{b}(\boldsymbol{\mu}) &= \mu_p \, \det(T(\mu_g)) \, T(\mu_g)^{-T} \, \mathbf{V}(\mu_g), & \sigma(\boldsymbol{\mu}) &= \det(T(\mu_g)), \\ f(\boldsymbol{\mu}) &= \det(T(\mu_g)) \, g(\mu_g), & \gamma(\boldsymbol{\mu}) &= \det(T(\mu_g)) \, \delta(\mu_g), \end{aligned} \tag{12}$$

where $\mathbf{V}$, g and δ correspond to the data $\mathbf{V}_0$, g_0 and δ_0 given on the real domain, respectively.

2 Finite Element Approximation: Stabilization

In this Section we consider the FE method for the numerical approximation of the hyperbolic advection–reaction PDE introduced in Section 1. With this aim we add suitable stabilization terms to the weak form of the problem according to the SDFE method (see e.g. [7, 8, 19, 28]). Moreover, we report an a priori FE error estimate and some estimates which we adopt in Section 3.2 for the a priori RB error estimate.

2.1 Stabilization: the SDFE method

We introduce now the SDFE method for the numerical approximation of the abstract problem of Section 1.1, as proposed in [7] and discussed in [28].
Let us indicate with $\{K\}$ the triangular elements of a quasi–uniform unstructured mesh $\mathcal{T}_h$ of the domain Ω, s.t. $\cup_{K\in\mathcal{T}_h} = \overline{\Omega}$, and h as $h := \max_{K\in\mathcal{T}_h} \mathrm{diam}(K)$. For the FE approximation we use piecewise linear basis functions on $K \in \mathcal{T}_h$ and we define the space $X_h := \left\{w \in C^0(\overline{\Omega}) \ : \ w_{|K} \in \mathbb{P}^1(K) \ \ \forall K \in \mathcal{T}_h\right\}$.
The stabilized discrete weak form of the problem (1) reads:

$$\text{find} \ \ \phi_h(\boldsymbol{\mu}) \in \mathcal{V}_h \quad : \quad A_h(\phi_h(\boldsymbol{\mu}), v_h; \boldsymbol{\mu}) = F_h(v_h; \boldsymbol{\mu}) \qquad \forall v_h \in \mathcal{V}_h, \ \ \forall \boldsymbol{\mu} \in \mathcal{D}, \tag{13}$$

where $\mathcal{V}_h \subset \mathcal{V}$ is the FE space, being $\mathcal{V}_h := \{w \in X_h \ : \ w(\mathbf{x}) = 0 \ \ \forall \mathbf{x} \in \Gamma_D\}$, and, from Eq.(3):

$$\begin{aligned} A_h(w, v; \boldsymbol{\mu}) \quad &:= \quad A(w, v; \boldsymbol{\mu}) \ + \ \varepsilon_h(h, \boldsymbol{\mu}) \int_\Omega \nabla w \cdot \nabla v \ d\Omega \\ &\quad + \ \delta_h(h, \boldsymbol{\mu}) \int_\Omega (\mathbf{b}(\boldsymbol{\mu}) \cdot \nabla w) \ \ (\mathbf{b}(\boldsymbol{\mu}) \cdot \nabla v) \ \ d\Omega \\ &\quad + \ \delta_h(h, \boldsymbol{\mu}) \int_\Omega w \ \mathbf{b}(\boldsymbol{\mu}) \cdot \nabla v \ d\Omega, \\ F_h(v; \boldsymbol{\mu}) \quad &:= \quad F(v; \boldsymbol{\mu}) \ + \ \delta_h(h, \boldsymbol{\mu}) \int_\Omega f(\boldsymbol{\mu}) \ \mathbf{b}(\boldsymbol{\mu}) \cdot \nabla v \ d\Omega. \end{aligned} \tag{14}$$

The coefficients $\varepsilon_h(h, \boldsymbol{\mu})$ and $\delta_h(h, \boldsymbol{\mu})$ are chosen as in [7, 28]:

$$\varepsilon_h(h, \boldsymbol{\mu}) := C_\varepsilon(\boldsymbol{\mu}) h^{3/2}, \qquad \delta_h(h, \boldsymbol{\mu}) := C_\delta(\boldsymbol{\mu}) h, \tag{15}$$

and are considered "small". By indicating with V and L the measure units of the advection field $\mathbf{b}(\boldsymbol{\mu})$ and the length respectively, we observe that, for dimensional reasons applied to the weak form (13), $[C_\varepsilon(\boldsymbol{\mu})] = V/L^{1/2}$ and $[C_\delta(\boldsymbol{\mu})] = 1/V$. For example, for the Problems 1 and 2 of Sections 1.2 and 1.3, we choose $C_\varepsilon(\boldsymbol{\mu}) = c_\varepsilon \mu_p$ and $C_\delta(\boldsymbol{\mu}) = c_\delta/\mu_p$.
Let us observe that the continuous stabilized version of the problem (13) would read:

$$\text{find} \ \ \phi_c(\boldsymbol{\mu}) \in \mathcal{V} \quad : \quad A_h(\phi_c(\boldsymbol{\mu}), v_c; \boldsymbol{\mu}) = F_h(v_c; \boldsymbol{\mu}) \qquad \forall v_c \in \mathcal{V}, \ \ \forall \boldsymbol{\mu} \in \mathcal{D}, \tag{16}$$

where the continuous solution $\phi_c(\boldsymbol{\mu}) \in \mathcal{V}$ of the stabilized problem differs from the continuous solution $\phi(\boldsymbol{\mu}) \in \mathcal{V}$ of the original problem in weak form (2).
Let us notice that the stabilization acts only on the weak form (2), but not directly on the functional output (5). The output corresponding to the FE solution is:

$$s_h(\boldsymbol{\mu}) := L(\phi_h(\boldsymbol{\mu}); \boldsymbol{\mu}). \tag{17}$$

Remark 2.1 *The stabilized advection–reaction problem (13) corresponds to an elliptic PDE, for which boundary conditions are necessary on the whole boundary $\partial\Omega$ and not only on Γ_D. The choice made for the FE space $\mathcal{V}_h$ consists in assuming implicitly homogeneous Neumann condition on Γ_N.*

Let us observe that, due to the affine decomposition assumptions made in Section 1.1 for $\mathbf{b}(\boldsymbol{\mu})$, $\sigma(\boldsymbol{\mu})$ and $f(\boldsymbol{\mu})$, even for the stabilized problem, as the "original" one (see Eq.(4)), the affine decomposition property holds, i.e.:

$$A_h(w,v;\boldsymbol{\mu}) = \sum_{q=1}^{Q_h} \vartheta_{hq}(\boldsymbol{\mu}) A_{hq}(w,v), \qquad F_h(v;\boldsymbol{\mu}) := \sum_{q=1}^{Q_h^F} \vartheta_{hq}^F(\boldsymbol{\mu}) F_{hq}(v). \tag{18}$$

for some $Q_h, Q_h^F \in \mathbb{N}$. By writing the FE solution as $\phi_h(\boldsymbol{\mu}) = \sum_{j=1}^{N_h} \phi_{hj}(\boldsymbol{\mu})\varphi_j$, being φ_j the FE lagrangian basis function associated with the FE space $\mathcal{V}_h$ and N_h the number of the nodes of the triangulation $\mathcal{T}_h$; it follows that the FE problem corresponds to the following linear system:

$$\text{find } \boldsymbol{\phi}_h(\boldsymbol{\mu}) \in \mathbb{R}^{N_h} \ : \ A_h(\boldsymbol{\mu})\boldsymbol{\phi}_h(\boldsymbol{\mu}) = \mathbf{F}_h(\boldsymbol{\mu}), \tag{19}$$

where $(\boldsymbol{\phi}_h(\boldsymbol{\mu}))_i = \phi_{hi}(\boldsymbol{\mu})$; the matrix $A_h(\boldsymbol{\mu}) \in \mathbb{R}^{N_h \times N_h}$ and the vector $\mathbf{F}_h(\boldsymbol{\mu}) \in \mathbb{R}^{N_h}$ are defined respectively as $A_h(\boldsymbol{\mu}) := \sum_{q=1}^{Q_h} \vartheta_{hq}(\boldsymbol{\mu}) A_{hq}$ with $(A_{hq})_{i,j} := A_{hq}(\varphi_i, \varphi_j)$ and $\mathbf{F}_h(\boldsymbol{\mu}) := \sum_{q=1}^{Q_h^F} \vartheta_q^F(\boldsymbol{\mu}) \mathbf{F}_{hq}$ with $(\mathbf{F}_{hq})_i := F_q(\varphi_i)$. By recalling Eq.s (5), (7) and (17) and by defining the vector $\mathbf{L}_h(\boldsymbol{\mu}) \in \mathbb{R}^{N_h}$ as $\mathbf{L}_h(\boldsymbol{\mu}) := \sum_{q=1}^{Q^L} \vartheta_q^L(\boldsymbol{\mu}) \mathbf{L}_{hq}$ with $(\mathbf{L}_{hq})_i := L_q(\varphi_i)$, the output can finally be computed as $s_h(\boldsymbol{\mu}) = \boldsymbol{\phi}_h(\boldsymbol{\mu}) \cdot \mathbf{L}_h(\boldsymbol{\mu})$.

Let us now introduce the stabilized *dual problem* associated with the weak form (13) and the output (5):

$$\text{find } \ \psi(\boldsymbol{\mu}) \in \mathcal{V} \ : \ A_h(v, \psi(\boldsymbol{\mu}); \boldsymbol{\mu}) = -L(v;\boldsymbol{\mu}) \qquad \forall v \in \mathcal{V}, \ \ \forall \boldsymbol{\mu} \in \mathcal{D} \tag{20}$$

and the corresponding discrete problem:

$$\text{find } \ \psi_h(\boldsymbol{\mu}) \in \mathcal{V}_h \ : \ A_h(v_h, \psi_h(\boldsymbol{\mu}); \boldsymbol{\mu}) = -L(v_h;\boldsymbol{\mu}) \qquad \forall v_h \in \mathcal{V}_h, \ \ \forall \boldsymbol{\mu} \in \mathcal{D}. \tag{21}$$

For the sake of simplicity, we have avoided the subscript 'c' for $\psi(\boldsymbol{\mu}) \in \mathcal{V}$ in Eq.(20); we stress the fact that Eq.(20) does not represent the continuous dual problem, but only the continuous version of the stabilized one.
In analogy with the primal FE problem, the FE dual solution corresponds to the solution of the following linear system:

$$\text{find } \boldsymbol{\psi}_h(\boldsymbol{\mu}) \in \mathbb{R}^{N_h} \ : \ A_h(\boldsymbol{\mu})^T \boldsymbol{\psi}_h(\boldsymbol{\mu}) = -\mathbf{L}_h(\boldsymbol{\mu}), \tag{22}$$

where $(\boldsymbol{\psi}_h(\boldsymbol{\mu}))_i = \psi_{hi}(\boldsymbol{\mu})$, being $\psi_h(\boldsymbol{\mu}) = \sum_{j=1}^{N_h} \psi_{hj}(\boldsymbol{\mu})\psi_j$. In the same manner as the stabilized primal problem (13), also the dual one admits an affine decomposition, due to the assumption made for $\gamma(\boldsymbol{\mu})$ in Section 1.1.

Remark 2.2 *Let us now consider an advection–diffusion–reaction problem with diffusion coefficient ε "small", s.t. the solution of this elliptic problem assumes a hyperbolic behavior. Moreover, let us assume an homogeneous Dirichlet condition on the whole boundary $\partial\Omega$. The FE problem should be stabilized in order to avoid numerical instabilities. If we consider the SDFE method, the stabilized problem assumes the form (13), where we have neglected the diffusion term ε, being $\varepsilon \ll \varepsilon_h$ due to the hypothesis ε "small". Let us observe that in this case we have $\mathcal{V}_h := \{w \in X_h \ : \ w(\mathbf{x}) = 0 \ \ \forall \mathbf{x} \in \partial\Omega\}$. We refer to this problem as Problem 1(bis).*

2.2 A priori FE error estimate

In this Section we consider the a priori FE error estimate associated with the solution of the stabilized problem (13) according to the SDFE method and the output. First of all, we provide the a priori FE error estimate for the Problem 1(bis) (see Remark 2.2); then, we some estimates for the general stabilized problem of Section 2.1 are reported.

2.2.1 Problem 1(bis)

By considering the Problem 1(bis) described in Remark 2.2, we shortly recall here the a priori error estimate of the solution of the problem (13) and the corresponding output (for more details, see [3, 28]).
Let us define the following norm, which depends on the parameter vector $\boldsymbol{\mu}$:

$$|||v|||^2 := \varepsilon_h(h,\boldsymbol{\mu})||\nabla v||^2 + \delta_h(h,\boldsymbol{\mu})||\mathbf{b}(\boldsymbol{\mu})\cdot\nabla v||^2 + ||v||^2, \tag{23}$$

where $||\cdot||$ indicates the usual $L^2(\Omega)$ norm ([9]). It is possible to show that the stabilized Problem 1(bis) admits an unique solution, being the form $A_h(\cdot,\cdot;\boldsymbol{\mu})$ bilinear, continuous and coercive and the functional $F_h(\cdot;\boldsymbol{\mu})$ linear and continuous. The continuity of the form $A_h(\cdot,\cdot;\boldsymbol{\mu})$ follows from:

$$|A_h(w_h,v_h;\boldsymbol{\mu})| \leq \left[\max\{1,||\sigma(\boldsymbol{\mu})||_\infty\} + (\delta_h(h,\boldsymbol{\mu}))^{-1/2}\right]\ |||w_h|||\,|||v_h||| \qquad \forall w_h, v_h \in \mathcal{V}_h, \tag{24}$$

while the coercivity from:

$$A_h(v_h,v_h;\boldsymbol{\mu}) \geq \alpha(\boldsymbol{\mu})\ |||v_h|||^2 \qquad \forall v_h \in \mathcal{V}_h, \tag{25}$$

where $\alpha(\boldsymbol{\mu})$ is the coercivity constant:

$$\alpha(\boldsymbol{\mu}) := \min\{1, ||\sigma(\boldsymbol{\mu})||_\infty\}. \tag{26}$$

For the sake of simplicity, $||\sigma(\boldsymbol{\mu})||_\infty$ stands for $||\sigma(\boldsymbol{\mu})||_{L^\infty(\Omega)}$. The same considerations hold also for the corresponding stabilized dual problem, which admits an unique solution. By defining the error $e_h(\boldsymbol{\mu}) \in \mathcal{V}_h$ as $e_h(\boldsymbol{\mu}) := \phi(\boldsymbol{\mu}) - \phi_h(\boldsymbol{\mu})$, we obtain the following a priori error estimate (see [3, 28]):

$$|||e_h(\boldsymbol{\mu})||| \leq C(\boldsymbol{\mu})h^{3/2}|\phi(\boldsymbol{\mu})|_{H^2(\Omega} \qquad \forall \boldsymbol{\mu} \in \mathcal{D}, \tag{27}$$

with $C(\boldsymbol{\mu})$ depending on $\boldsymbol{\mu}$, $||\mathbf{b}(\boldsymbol{\mu})||$ and $||\sigma(\boldsymbol{\mu})||_\infty$; the estimate (27) shows the convergence rate 3/2 in h. If we consider the Problem 1(bis), the estimate (27) reads:

$$|||e_h(\boldsymbol{\mu})||| \leq c\ \mu^{1/2}\ h^{3/2}|\phi(\boldsymbol{\mu})|_{H^2(\Omega)} \qquad \forall \mu \in \mathcal{D}, \tag{28}$$

for some $c \in \mathbb{R}$, which does not depend on μ.
By using similar arguments, it is possible to provide an a priori FE error estimate also for the dual problem (21), which, if $\psi(\boldsymbol{\mu}) \in H^2(\Omega) \cap \mathcal{V}$, reads:

$$|||e_h^{du}(\boldsymbol{\mu})||| \leq C^{du}(\boldsymbol{\mu})h^{3/2}|\psi(\boldsymbol{\mu})|_{H^2(\Omega)} \qquad \forall \boldsymbol{\mu} \in \mathcal{D}, \tag{29}$$

where $e_h^{du}(\boldsymbol{\mu}) := \psi(\boldsymbol{\mu}) - \psi_h(\boldsymbol{\mu})$ and $C^{du}(\boldsymbol{\mu})$ depends on $\boldsymbol{\mu}$ and the data of the problem.

In order to provide the a priori FE error estimate for the output $s(\boldsymbol{\mu})$, we introduce the corrected (deflated) output:

$$\widetilde{s}_h(\boldsymbol{\mu}) := s_h(\boldsymbol{\mu}) - \delta s_h(\boldsymbol{\mu}) \qquad \text{with}\ \ \delta s_h(\boldsymbol{\mu}) := -\varepsilon_h(h,\boldsymbol{\mu})\int_\Omega \nabla\phi_h(\boldsymbol{\mu})\cdot\nabla\psi_h\ d\Omega. \tag{30}$$

We obtain the following a priori FE error estimate [3]:

$$|s(\boldsymbol{\mu}) - \widetilde{s}_h(\boldsymbol{\mu})| \leq C^s(h,\boldsymbol{\mu}) h^{5/2} |\phi(\boldsymbol{\mu})|_{H^2(\Omega)} |\psi(\boldsymbol{\mu})|_{H^2(\Omega)}, \tag{31}$$

where the constant $C^s(h,\boldsymbol{\mu}) \in \mathbb{R}$ does not affect the convergence order in h, being: $C^s(h,\boldsymbol{\mu}) := C_1^s(\boldsymbol{\mu}) \left\{1 + C_2^s(\boldsymbol{\mu}) h^{1/2}\right\}$, with the constants $C_1^s(\boldsymbol{\mu})$ and $C_1^s(\boldsymbol{\mu})$ not dependent on h. In particular, for Problem 1(bis), we have for $h \to 0$:

$$|s(\boldsymbol{\mu}) - \widetilde{s}_h(\boldsymbol{\mu})| \leq c_s \mu^{3/2} h^{5/2} |\phi(\boldsymbol{\mu})|_{H^2(\Omega)} |\psi(\boldsymbol{\mu})|_{H^2(\Omega)}, \tag{32}$$

for some $c_s \in \mathbb{R}$, which does not depend neither on h nor on μ.

2.2.2 The general case

We return now the general problem introduced in Section 1.1; however, we observe that in this case it is not straightforward to provide a priori FE error estimates for the primal and dual solutions and the output in the same manner as made for the Problem 1(bis), being $\Gamma_D \neq \partial\Omega$. However, we highlight here some estimates that we use in the following Sections for the analysis of the RB problem.
For the general case, we introduce the following norm:

$$|||v|||^2 := \varepsilon_h(h,\boldsymbol{\mu}) ||\nabla v||^2 + \delta_h(h,\boldsymbol{\mu}) ||\mathbf{b}(\boldsymbol{\mu}) \cdot \nabla v||^2 + ||v||^2 + \frac{1 + \delta_h(h,\boldsymbol{\mu})}{2} ||(\mathbf{b}(\boldsymbol{\mu}) \cdot \hat{\mathbf{n}})^{1/2} v||^2_{\Gamma_N}, \tag{33}$$

where $||\cdot||_{\Gamma_N} := ||\cdot||_{L(\Gamma_N)}$; the norm (23) is a particular case of the norm (33), when $\Gamma_N \equiv \emptyset$. We recall that $|||\cdot|||$ depends on $\boldsymbol{\mu}$. In analogy with Problem 1(bis), it is simple to prove the existence and uniqueness of the solution of the problem (13); in fact, the form (14) is coercive and continuous even with the new norm (see [3]). This last property follows from :

$$|A_h(w_h, v_h; \boldsymbol{\mu})| \leq \left[2 \max\{1, ||\sigma(\boldsymbol{\mu})||_\infty\} + (\delta_h(h,\boldsymbol{\mu}))^{-1/2}\right] \; |||w_h||| \; |||v_h|||, \tag{34}$$

which shows the continuity of the bilinear form $A_h(\cdot,\cdot;\boldsymbol{\mu})$.
Similarly, existence and uniqueness of the dual problem solution are ensured.

3 The Reduced Basis Method

In this Section we consider the RB method for the solution of the stabilized parametrized advection–reaction problem of Section 2 according to the "primal–dual" RB approach. We provide both the a priori and a posteriori RB error estimates and an adaptive algorithm for the choice of the samples for the basis generation.

3.1 The RB method for the stabilized problem

We recall here the RB method by referring to the stabilized problem of Section 2.1; in particular, we consider the "primal–dual" RB approach. For further details about the RB method and applications, see [5, 6, 11, 13, 14, 16, 20, 23, 26, 27].
Let us introduce the following set of parameters $\mathcal{S}_N^{pr} := \{\boldsymbol{\mu}_1^{pr}, \ldots, \boldsymbol{\mu}_N^{pr}\}$, with $\boldsymbol{\mu}_i^{pr} \in \mathcal{D}$, $\forall i = 1, \ldots, N^{pr}$, $N^{pr} \in \mathbb{N}$; the superscript "pr" is used to refer to the primal problem. The set of parameters $\boldsymbol{\mu}_i^{pr}$ and their number N^{pr} can be chosen in the space $\mathcal{D}$ according to the adaptive algorithm that we discuss in Section 3.4; other choices are possible

(see [13]). For each $\boldsymbol{\mu}_i^{pr} \in \mathcal{S}_N^{pr}$, we solve, by means of the FE element method, the stabilized primal problem (13), obtaining the corresponding discretized primal solutions $\phi_h(\boldsymbol{\mu}_i^{pr}) \in \mathcal{V}_h$. Then, we define the RB space associated with the primal problem:

$$\mathcal{V}_N^{pr} := \text{span}\,\{\xi_i := \phi_h(\boldsymbol{\mu}_i^{pr}) \;\; i = 1, \ldots, N^{pr}\} \tag{35}$$

and the RB primal problem:

$$\text{find } \phi_N(\boldsymbol{\mu}) \in \mathcal{V}_N^{pr} \;\; : \;\; A_h(\phi_N(\boldsymbol{\mu}), v_N; \boldsymbol{\mu}) = F_h(v_N; \boldsymbol{\mu}) \qquad \forall v_N \in \mathcal{V}_N^{pr}, \quad \forall \boldsymbol{\mu} \in \mathcal{D}, \tag{36}$$

where $A_h(\cdot, \cdot; \boldsymbol{\mu})$ and $F_h(\cdot; \boldsymbol{\mu})$ are defined in Eq.(14); we suppose that the solution $\phi_N(\boldsymbol{\mu})$ of the RB primal problem could be expressed as:

$$\phi_N(\boldsymbol{\mu}) = \sum_{j=1}^{N^{pr}} \phi_{Nj}(\boldsymbol{\mu}) \xi_j. \tag{37}$$

For the sake of simplicity, we have used the notation $\phi_N(\boldsymbol{\mu})$ to indicate the RB solution $\phi_{hN}(\boldsymbol{\mu})$ of the primal problem (36).

Remark 3.1 *From a numerical point of view, the discrete problem associated with (36) becomes more and more ill–conditioned with N^{pr} increasing in size, so affecting the accuracy of the RB solution. To overcome this difficulty, it is convenient to adopt an orthonormal basis for the generation of the RB space $\mathcal{V}_N^{pr}$; in particular we consider the Gram–Schmidt orthormalization with respect to the inner product $(\cdot, \cdot)$ induced by the norm $||\cdot||$ (see e.g. [13]). Let us indicate the new orthonormal basis for the RB space $\mathcal{V}_N^{pr}$ as $\{\varrho_i\}_{i=1}^{N^{pr}}$, which we compute according to the following procedure:*

$$\varrho_1 = \xi_1/||\xi_1||; \qquad z_i = \xi_i - \sum_{j=1}^{i-1} (\varrho_j, \xi_i)\varrho_j, \qquad \varrho_i = z_i/||z_i|| \qquad i = 2, \ldots, N^{pr}. \tag{38}$$

We obtain that $\mathcal{V}_N^{pr} = \text{span}\{\xi_i, \; i = 1, \ldots, N^{pr}\} = \text{span}\{\varrho_i, \; i = 1, \ldots, N^{pr}\}$. Let us notice that we will consider the orthonormal basis for the definition of our RB problem; however, for the sake of simplicity, we identify the basis $\{\xi_i\}_{i=1}^{N^{pr}}$ used in Eq.s (35) and (36) as the orthonormal basis $\{\varrho_i\}_{i=1}^{N^{pr}}$.

Owing to the assumption made in Section 2.1 concerning with the affine decomposition of $A_h(\cdot, \cdot; \boldsymbol{\mu})$ and $F_h(\cdot; \boldsymbol{\mu})$ (see Eq.(18)) and Eq.(37), Eq.(36) reads:

$$\begin{gathered} \text{find } \phi_{Nj}(\boldsymbol{\mu}) \quad j = 1, \ldots, N^{pr} \;\; : \\ \sum_{q=1}^{Q_h} \vartheta_{hq}(\boldsymbol{\mu}) A_{hq}(\xi_j, \xi_i) \phi_{Nj}(\boldsymbol{\mu}) = \sum_{q=1}^{Q_h^F} \vartheta_{hq}^F(\boldsymbol{\mu}) F_{hq}(\xi_i) \quad \forall i = 1, \ldots, N^{pr}, \quad \forall \boldsymbol{\mu} \in \mathcal{D}. \end{gathered} \tag{39}$$

which can be re–written in matricial notation as:

$$\text{find } \boldsymbol{\phi}_N(\boldsymbol{\mu}) \in \mathbb{R}^{N^{pr}} \;\; : \;\; A_N^{pr}(\boldsymbol{\mu}) \boldsymbol{\phi}_N(\boldsymbol{\mu}) = \mathbf{F}_N^{pr}(\boldsymbol{\mu}), \tag{40}$$

being the matrix $A_N^{pr}(\boldsymbol{\mu}) \in \mathbb{R}^{N^{pr} \times N^{pr}}$ and the vector $\mathbf{F}_N^{pr}(\boldsymbol{\mu}) \in \mathbb{R}^{N^{pr}}$ defined respectively as $A_N^{pr}(\boldsymbol{\mu}) := \sum_{q=1}^{Q_h} \vartheta_{hq}(\boldsymbol{\mu}) A_{Nq}^{pr}$ with $\left(A_{Nq}^{pr}\right)_{i,j} := A_{hq}(\xi_j, \xi_i)$ and $\mathbf{F}_N^{pr}(\boldsymbol{\mu}) :=$

$\sum_{q=1}^{Q_h^F} \vartheta_{hq}^F(\boldsymbol{\mu})\mathbf{F}_{Nq}$ with $\left(\mathbf{F}_{Nq}^{pr}\right)_i := F_{hq}(\xi_i)$. By recalling Eq.s (5), (8) and (37), it follows that:

$$s_N(\boldsymbol{\mu}) := L(\phi_N(\boldsymbol{\mu}); \boldsymbol{\mu}) = \boldsymbol{\phi}_N(\boldsymbol{\mu}) \cdot \mathbf{L}_N^{pr}(\boldsymbol{\mu}), \tag{41}$$

where the vector $\mathbf{L}_N^{pr}(\boldsymbol{\mu}) \in \mathbb{R}^{N^{pr}}$ is defined as $\mathbf{L}_N^{pr}(\boldsymbol{\mu}) := \sum_{q=1}^{Q^L} \vartheta_q^L(\boldsymbol{\mu})\mathbf{L}_{Nq}^{pr}$ with $\left(\mathbf{L}_{Nq}^{pr}\right)_i := L_q(\xi_i)$.

Similarly, it is possible to afford the dual RB problem.
Let us select a set of parameters $\mathcal{S}^{du} := \{\boldsymbol{\mu}_1^{du}, \ldots, \boldsymbol{\mu}_N^{du}\}$, with $\boldsymbol{\mu}_i^{du} \in \mathcal{D}$, $\forall i = 1, \ldots, N^{du}$, $N^{du} \in \mathbb{N}$; in this case the superscript 'du' refers to the dual problem.

Remark 3.2 *Let us observe that we consider the non–integrated primal and dual RB approach [13], for which, not only $N^{pr} \neq N^{du}$, but also the sets $\mathcal{S}^{pr}$ and $\mathcal{S}^{du}$ are composed by different parameters; this issue will be re–called and discussed in Section 3.4.3.*

By defining the RB space for the dual problem as:

$$\mathcal{V}_N^{du} := \text{span}\left\{\zeta_i := \psi_h(\boldsymbol{\mu}_i^{du}) \;\; i = 1, \ldots, N^{du}\right\}, \tag{42}$$

where $\psi_h(\boldsymbol{\mu}_i^{du})$ is the solution of the FE dual problem (21) corresponding to the parameter $\boldsymbol{\mu}_i^{du}$ and $\{\zeta_i\}_{i=1}^{N^{du}}$ is an orthonormal basis (see Remark 3.1). The dual RB problem reads:

$$\text{find } \psi_N(\boldsymbol{\mu}) \in \mathcal{V}_N^{du} \;:\; A_h(v_N, \psi_N(\boldsymbol{\mu}); \boldsymbol{\mu}) = -L(v_N; \boldsymbol{\mu}) \qquad \forall v_N \in \mathcal{V}_N^{du}, \quad \forall \boldsymbol{\mu} \in \mathcal{D}; \tag{43}$$

the dual RB solution can be written as:

$$\psi_N(\boldsymbol{\mu}) = \sum_{j=1}^{N^{du}} \psi_{Nj}(\boldsymbol{\mu})\zeta_j. \tag{44}$$

According to Eq.s (7), (18), (21), Eq.(43) can be expressed in matricial notation as:

$$\text{find } \boldsymbol{\psi}_N(\boldsymbol{\mu}) \in \mathbb{R}^{N^{du}} \;:\; A_N^{du}(\boldsymbol{\mu})\boldsymbol{\psi}_N(\boldsymbol{\mu}) = -\mathbf{L}_N^{du}(\boldsymbol{\mu}), \tag{45}$$

being the matrix $A_N^{du}(\boldsymbol{\mu}) \in \mathbb{R}^{N^{du} \times N^{du}}$ and the vector $\mathbf{L}_N^{du}(\boldsymbol{\mu}) \in \mathbb{R}^{N^{du}}$ defined respectively as: $A_N^{du}(\boldsymbol{\mu}) := \sum_{q=1}^{Q_h} \vartheta_{hq}(\boldsymbol{\mu})A_{Nq}^{du}$ with $\left(A_{Nq}^{du}\right)_{i,j} := A_{hq}(\zeta_i, \zeta_j)$ and $\mathbf{L}_N^{du}(\boldsymbol{\mu}) := \sum_{q=1}^{Q^L} \vartheta_q^L(\boldsymbol{\mu})\mathbf{L}_{Nq}$ with $\left(\mathbf{L}_{Nq}^{du}\right)_i := L_q(\zeta_i)$.

3.2 A priori RB error estimate

In this Section we discuss the a priori RB error estimates both for the primal and dual solutions and the output.
First of all, let us observe that the solution of the primal RB problem $\phi_N(\boldsymbol{\mu})$ belongs not only to $\mathcal{V}_N^{pr}$, but also to the FE space $\mathcal{V}_h$ ($\phi_N(\boldsymbol{\mu}) \in \mathcal{V}_N^{pr} \subset \mathcal{V}_h$); in the same manner the dual RB solution $\psi_N(\boldsymbol{\mu}) \in \mathcal{V}_N^{du} \subset \mathcal{V}_h$.
By recalling the coercivity property (25) of $A_h(\cdot, \cdot; \boldsymbol{\mu})$ w.r.t. the norm $|||\cdot|||$ of Eq.(33) (or Eq.(23) for Problem 1(bis)), it follows:

$$|||e_N^{pr}(\boldsymbol{\mu})|||^2 \leq \frac{1}{\min\{1, ||\sigma(\boldsymbol{\mu})||_\infty\}} A_h(e_N^{pr}(\boldsymbol{\mu}), e_N^{pr}(\boldsymbol{\mu}); \boldsymbol{\mu}) \tag{46}$$

where $e_N^{pr}(\boldsymbol{\mu}) := \phi_h(\boldsymbol{\mu}) - \phi_N(\boldsymbol{\mu})$ is the primal RB error, s.t. $e_N^{pr}(\boldsymbol{\mu} \in \mathcal{V}_h$. By observing from Eq.s (13) and (36) that, for the primal RB problem, the Galerkin orthogonality property holds:

$$A_h(e_N^{pr}(\boldsymbol{\mu}), v_N; \boldsymbol{\mu}) = 0 \qquad \forall v_N \in \mathcal{V}_N^{pr}, \tag{47}$$

the bilinear form $A_h(e_N^{pr}(\boldsymbol{\mu}), e_N^{pr}(\boldsymbol{\mu}); \boldsymbol{\mu})$ can be written as:

$$A_h(e_N^{pr}(\boldsymbol{\mu}), e_N^{pr}(\boldsymbol{\mu}); \boldsymbol{\mu}) = A_h(e_N^{pr}(\boldsymbol{\mu}), \phi_h(\boldsymbol{\mu}) - v_N; \boldsymbol{\mu}) \qquad \forall v_N \in \mathcal{V}_N^{pr}, \tag{48}$$

being $\phi_h(\boldsymbol{\mu}) - v_N \in \mathcal{V}_N^{pr}$. By applying the inequality (34) to Eq.(48), recalling Eq.(46) and simplifying the term $|||e_N^{pr}(\boldsymbol{\mu})|||$ both on the l.h.s and r.h.s of the inequality, we have:

$$|||e_N^{pr}(\boldsymbol{\mu})||| \leq \frac{2\max\{1, ||\sigma(\boldsymbol{\mu})||_\infty\} + (\delta_h(h, \boldsymbol{\mu}))^{-1/2}}{\min\{1, ||\sigma(\boldsymbol{\mu})||_\infty\}} |||\phi_h(\boldsymbol{\mu}) - v_N||| \qquad \forall v_N \in \mathcal{V}_N^{pr}. \tag{49}$$

From Eq.s (15) and (49) it follows the a priori primal RB error estimate:

$$|||e_N^{pr}(\boldsymbol{\mu})||| \leq \Xi(\boldsymbol{\mu}) \inf_{v_N \in \mathcal{V}_N^{pr}} |||\phi_h(\boldsymbol{\mu}) - v_N||| \qquad \forall \boldsymbol{\mu} \in \mathcal{D}, \tag{50}$$

with:

$$\Xi(\boldsymbol{\mu}) := \frac{2\max\{1, ||\sigma(\boldsymbol{\mu})||_\infty\} + (C_\delta(\boldsymbol{\mu})h)^{-1/2}}{\min\{1, ||\sigma(\boldsymbol{\mu})||_\infty\}}. \tag{51}$$

In the special case of Problem 1, the estimate (50) holds with:

$$\Xi(\mu) = 2 + \left(\frac{\mu}{c_\delta h}\right)^{1/2}. \tag{52}$$

Similarly, the following a priori RB error estimate for the dual problem holds:

$$|||e_N^{du}(\boldsymbol{\mu})||| \leq \Xi(\boldsymbol{\mu}) \inf_{v_N \in \mathcal{V}_N^{du}} |||\psi_h(\boldsymbol{\mu}) - v_N||| \qquad \forall \boldsymbol{\mu} \in \mathcal{D}, \tag{53}$$

where $e_N^{du}(\boldsymbol{\mu}) := \psi_h(\boldsymbol{\mu}) - \psi_N(\boldsymbol{\mu})$.

By means of Eq.s (5), (17), (21) and (41) and the Galerkin orthogonality property (47), we have:

$$s_h(\boldsymbol{\mu}) - s_N(\boldsymbol{\mu}) = L(e_N^{pr}(\boldsymbol{\mu}); \boldsymbol{\mu}) = -A_h(e_N^{pr}(\boldsymbol{\mu}), e_N^{du}(\boldsymbol{\mu}); \boldsymbol{\mu}), \tag{54}$$

which, according to the inequality (34), leads to the following a priori RB error estimate for the output:

$$|s_h(\boldsymbol{\mu}) - s_N(\boldsymbol{\mu})| \leq \Xi(\boldsymbol{\mu})^3 \left(\inf_{v_N \in \mathcal{V}_N^{pr}} |||\phi_h(\boldsymbol{\mu}) - v_N|||\right) \left(\inf_{w_N \in \mathcal{V}_N^{du}} |||\psi_h(\boldsymbol{\mu}) - w_N|||\right). \tag{55}$$

3.3 A posteriori RB error estimate

In this Section we discuss the a posteriori RB error estimate for the output; for further details refer to [11, 13, 24]. We will use this result in Section 3.4 for the choice of the samples sets $\mathcal{S}_N^{pr}$ and $\mathcal{S}_N^{du}$.

Let us define the RB residuals associated with the primal and dual problems by recalling respectively Eq.s (13) and (21):

$$R_N^{pr}(v; \boldsymbol{\mu}) := F_h(v; \boldsymbol{\mu}) - A_h(\phi_N(\boldsymbol{\mu}), v; \boldsymbol{\mu}) = A_h(e_N^{pr}(\boldsymbol{\mu}), v; \boldsymbol{\mu}), \tag{56}$$

$$R_N^{du}(v;\boldsymbol{\mu}) := -L(v;\boldsymbol{\mu}) - A_h(v,\psi_N(\boldsymbol{\mu});\boldsymbol{\mu}) = A_h(v,e_N^{du}(\boldsymbol{\mu});\boldsymbol{\mu}), \tag{57}$$

with $v \in \mathcal{V}_h$. Moreover, we define the corrected RB output (deflated) [24]:

$$\widetilde{s}_N(\boldsymbol{\mu}) := s_N(\boldsymbol{\mu}) - R_N^{pr}(\psi_N(\boldsymbol{\mu});\boldsymbol{\mu}) \tag{58}$$

and we express the error with respect the corrected RB output as:

$$s_h(\boldsymbol{\mu}) - \widetilde{s}_N(\boldsymbol{\mu}) = -R_N^{pr}(e_N^{du}(\boldsymbol{\mu});\boldsymbol{\mu}). \tag{59}$$

By introducing the dual norm of $|||\cdot|||$ (see e.g. [9]), which we indicate as $|||\cdot|||_*$, the following inequality holds:

$$|s_h(\boldsymbol{\mu}) - \widetilde{s}_N(\boldsymbol{\mu})| \leq |||R_N^{pr}(\cdot;\boldsymbol{\mu})|||_* \; |||e_N^{du}(\boldsymbol{\mu})|||, \tag{60}$$

where:

$$|||R_N^{pr}(\cdot;\boldsymbol{\mu})|||_* := \sup_{v_h \in \mathcal{V}_h \setminus \{0\}} \frac{R_N^{pr}(v_h;\boldsymbol{\mu})}{|||v_h|||} \qquad \forall \boldsymbol{\mu} \in \mathcal{D}. \tag{61}$$

For the computation of the dual norms of the residual refer to [13, 24].
By introducing the parametrized Babŭska *inf–sup* stability constant (see [1]) $\beta(\boldsymbol{\mu})$:

$$\beta(\boldsymbol{\mu}) := \inf_{w_h \in \mathcal{V}_h \setminus \{0\}} \sup_{v_h \in \mathcal{V}_h \setminus \{0\}} \frac{A_h(w_h,v_h;\boldsymbol{\mu})}{|||w_h||| \; |||v_h|||} \qquad \forall \boldsymbol{\mu} \in \mathcal{D}, \tag{62}$$

and by observing from Eq.(57) that:

$$\beta(\boldsymbol{\mu})|||e_N^{du}(\boldsymbol{\mu})|||^2 \leq R_N^{du}(e_N^{du}(\boldsymbol{\mu});\boldsymbol{\mu}) \leq |||R_N^{du}(\cdot;\boldsymbol{\mu})|||_* \; |||e_N^{du}(\boldsymbol{\mu})||| \qquad \forall \boldsymbol{\mu} \in \mathcal{D}, \tag{63}$$

it follows:

$$|||e_N^{du}(\boldsymbol{\mu})||| \leq \frac{1}{\beta(\boldsymbol{\mu})}|||R_N^{du}(\cdot;\boldsymbol{\mu})|||_* \qquad \forall \boldsymbol{\mu} \in \mathcal{D}. \tag{64}$$

Due to Eq.s (60) and (64), the following a posteriori RB error estimate for the deflated output holds:

$$|s_h(\boldsymbol{\mu}) - \widetilde{s}_N(\boldsymbol{\mu})| \leq \Delta_N(\boldsymbol{\mu}) \qquad \forall \boldsymbol{\mu} \in \mathcal{D}. \tag{65}$$

where $\Delta_N(\boldsymbol{\mu}) := \Delta_N^{pr}(\boldsymbol{\mu}) \; \Delta_N^{du}(\boldsymbol{\mu})$, with:

$$\Delta_N^{pr}(\boldsymbol{\mu}) := \frac{1}{\sqrt{\beta(\boldsymbol{\mu})}}|||R_N^{pr}(\cdot;\boldsymbol{\mu})|||_*, \qquad \Delta_N^{du}(\boldsymbol{\mu}) := \frac{1}{\sqrt{\beta(\boldsymbol{\mu})}}|||R_N^{du}(\cdot;\boldsymbol{\mu})|||_*. \tag{66}$$

Remark 3.3 *Being the bilinear form $A_h(\cdot,\cdot;\boldsymbol{\mu})$ (14) coercive (Eq.(25)), the parametrized inf–sup constant (62) is positive $\beta(\boldsymbol{\mu}) > 0$ $\forall \boldsymbol{\mu} \in \mathcal{D}$, for which the a posteriori estimate (65) holds.*

Remark 3.4 *In order to make use of the a posteriori RB error estimate (65), we need the expression of $\beta(\boldsymbol{\mu})$ $\forall \boldsymbol{\mu} \in \mathcal{D}$; however, this is possible only in some particular cases. A possible solution consists in replacing $\beta(\boldsymbol{\mu})$ by a lower–bound $\beta_{LB}(\boldsymbol{\mu}) \leq \beta(\boldsymbol{\mu})$ $\forall \boldsymbol{\mu} \in \mathcal{D}$, which allows sufficiently and accurate approximations of $\beta(\boldsymbol{\mu})$ (see [24]). An other possibility arises by observing that, for a coercive problem, $\beta(\boldsymbol{\mu}) \geq \alpha(\boldsymbol{\mu})$, $\forall \boldsymbol{\mu} \in \mathcal{D}$, being $\alpha(\boldsymbol{\mu})$ the coercivity constant (26), for which we could assume $\beta_{LB}(\boldsymbol{\mu}) = \alpha(\boldsymbol{\mu}) = \min\{1, ||\sigma(\boldsymbol{\mu})||_\infty\}$. However, for problems with dominating transport regimes, the choice $\beta_{LB}(\boldsymbol{\mu}) = \alpha(\boldsymbol{\mu})$ could lead to excessively pessimistic approximations of $\beta(\boldsymbol{\mu})$, which affect the sharpness of the a posteriori RB estimate (65).*

As anticipated, the a posteriori RB estimate (65) should be reliable, in the sense that the error is bounded by the estimator, but also sharp, i.e. the error and the bound should be close each other, in order to avoid too pessimistic RB error estimates. To evaluate the sharpness property of the estimator $\Delta_N(\boldsymbol{\mu})$, let us introduce the following indicator (see [13]), regarded as *effectivity index*:

$$\eta_N := \frac{\sup_{\boldsymbol{\mu}\in\mathcal{D}} \Delta_N(\boldsymbol{\mu})}{\sup_{\boldsymbol{\mu}\in\mathcal{D}} |s_h(\boldsymbol{\mu}) - \widetilde{s}_N(\boldsymbol{\mu})|}, \tag{67}$$

which, according to the reliability property, should be greater than (or equal to) one ($\eta_N \geq 1$), but as close as possibile to 1 due to the sharpness property.

3.4 Numerical solution: offline–online computational procedure and adaptive algorithm

In this Section we discuss the details concerning with the numerical solution of the RB problem. We highlight the importance of the offline–online decomposition of the computational procedure for the RB problem and we provide an adaptive algorithm for the choice of the primal and dual samples sets by using a minimization criterium of online computational costs. See also [11, 13, 14].

3.4.1 Numerical issues

Firstly, we discuss some issues related to the numerical solution of the RB problem. The norm $|||\cdot|||$ of Eq.s (23) or (33) depends on the parameter $\boldsymbol{\mu} \in \mathbf{D}$; however, for computational reasons, it is convenient to fix a sample $\overline{\boldsymbol{\mu}} \in \mathcal{D}$ for which the norm is evaluated, s.t. the norms (23) and (33) become respectively:

$$|||v|||^2_{\overline{\boldsymbol{\mu}}} := \varepsilon_h(h,\overline{\boldsymbol{\mu}})||\nabla v||^2 + \delta_h(h,\overline{\boldsymbol{\mu}})||\mathbf{b}(\overline{\boldsymbol{\mu}})\cdot\nabla v||^2 + ||v||^2,$$

$$|||v|||^2_{\overline{\boldsymbol{\mu}}} := \varepsilon_h(h,\overline{\boldsymbol{\mu}})||\nabla v||^2 + \delta_h(h,\overline{\boldsymbol{\mu}})||\mathbf{b}(\overline{\boldsymbol{\mu}})\cdot\nabla v||^2 + ||v||^2 + \frac{1+\delta_h(h,\overline{\boldsymbol{\mu}})}{2}||(\mathbf{b}(\overline{\boldsymbol{\mu}})\cdot\hat{\mathbf{n}})^{1/2}v||^2_{\Gamma_N}. \tag{68}$$

This does not affect the a priori FE and RB error estimates (see Sections.s 2.2.1, 2.2.2 and 3.2) and the a posteriori RB estimate (see Section 3.3): simply, the quantities related to the parametrical "fixed" norm should be recomputed according to $|||\cdot|||_{\overline{\boldsymbol{\mu}}}$. For example, the inf–sup constant $\beta(\boldsymbol{\mu})$ (62), defined w.r.t the "fixed" norm reads:

$$\overline{\beta}(\boldsymbol{\mu}) := \inf_{w_h\in\mathcal{V}_h\setminus\{0\}} \sup_{v_h\in\mathcal{V}_h\setminus\{0\}} \frac{A_h(w_h,v_h;\boldsymbol{\mu})}{|||w_h|||_{\overline{\boldsymbol{\mu}}}\,|||v_h|||_{\overline{\boldsymbol{\mu}}}} \qquad \forall\boldsymbol{\mu}\in\mathcal{D}. \tag{69}$$

As anticipated in Remark 3.4, we need the expression of $\overline{\beta}(\boldsymbol{\mu})$ or of a lower bound. However, for the evaluation of $\overline{\beta}(\boldsymbol{\mu})$ we use a composite linear polinomial interpolant ([18]) defined on the parameter space $\mathcal{D}$:

$$\widetilde{\beta}(\boldsymbol{\mu}) := \sum_{m=1}^{K} \overline{\beta}(\boldsymbol{\mu}_m)\Pi_m(\boldsymbol{\mu}), \tag{70}$$

being $\{\Pi_m(\boldsymbol{\mu})\}_{m=1}^K$ the basis functions associated with the linear interpolant and $\{\boldsymbol{\mu}_m\}_{m=1}^K$ the samples, chosen in $\mathcal{D}$, being K the number of samples. The choice of the samples $\{\boldsymbol{\mu}_m\}_{m=1}^K$ and K is made by means of inspection of the function $\overline{\beta}(\boldsymbol{\mu})$ for $\boldsymbol{\mu}\in\mathcal{D}$.

From this it follows that the a posteriori RB estimate (65) reads now:

$$|s_h(\boldsymbol{\mu}) - \widetilde{s}_N(\boldsymbol{\mu})| \leq \overline{\Delta}_N(\boldsymbol{\mu}) \qquad \forall \boldsymbol{\mu} \in \mathcal{D}. \tag{71}$$

where $\overline{\Delta}_N(\boldsymbol{\mu}) := \overline{\Delta}_N^{pr}(\boldsymbol{\mu})\ \overline{\Delta}_N^{du}(\boldsymbol{\mu})$, with:

$$\overline{\Delta}_N^{pr}(\boldsymbol{\mu}) := \frac{1}{\sqrt{\widetilde{\beta}(\boldsymbol{\mu})}} |||R_N^{pr}(\cdot;\boldsymbol{\mu})|||_{\overline{\boldsymbol{\mu}}*}, \qquad \overline{\Delta}_N^{du}(\boldsymbol{\mu}) := \frac{1}{\sqrt{\widetilde{\beta}(\boldsymbol{\mu})}} |||R_N^{du}(\cdot;\boldsymbol{\mu})|||_{\overline{\boldsymbol{\mu}}*}, \tag{72}$$

being $|||\cdot|||_{\overline{\boldsymbol{\mu}}*}$ the dual norm associated with $|||\cdot|||_{\overline{\boldsymbol{\mu}}}$.
The RB problems make use of the parameter $\boldsymbol{\mu}$ chosen in the space $\mathcal{D}$. However, for computational reasons, the research of the RB samples sets $\mathcal{S}_N^{pr}$, $\mathcal{S}_N^{du}$ must be restricted to a discrete subset $\overline{\mathcal{D}} \subset \mathcal{D}$ with a number of samples $\overline{N}$ "sufficiently great". In order to evaluate the RB error, it is convenient to define the following indicators for the maximum and minimum output errors for any given N^{pr} and N^{du}:

$$E_N^{max} := \max_{\boldsymbol{\mu} \in \overline{\mathcal{D}}} |s_h(\boldsymbol{\mu}) - \widetilde{s}_N(\boldsymbol{\mu})|, \qquad E_N^{mean} := \frac{1}{\overline{N}} \left(\sum_{\boldsymbol{\mu} \in \overline{\mathcal{D}}} |s_h(\boldsymbol{\mu}) - \widetilde{s}_N(\boldsymbol{\mu})| \right). \tag{73}$$

In similar way, the effectivity index η_N (67) should be modified in:

$$\overline{\eta}_N := \frac{\max\limits_{\boldsymbol{\mu} \in \overline{\mathcal{D}}} \Delta_N(\boldsymbol{\mu})}{\max\limits_{\boldsymbol{\mu} \in \overline{\mathcal{D}}} |s_h(\boldsymbol{\mu}) - \widetilde{s}_N(\boldsymbol{\mu})|}. \tag{74}$$

3.4.2 Offline–online computational procedure

The rapid answer of the RB method in a many query input–output context is highlighted if the RB problem is solved by means of an appropriate the offline–online decomposition procedure.

In the *offline* step we define the RB spaces once time the sets $\mathcal{S}_N^{pr}$, $\mathcal{S}_N^{du}$ are given. This choice is performed according to the adaptive algorithm, which we describe in Section 3.4.3. Then we build the RB orthonormal basis $\{\xi_i\}_{i=1}^{N^{pr}}$, $\{\zeta_i\}_{i=1}^{N^{du}}$ by solving the primal and dual FE problems and finally we assemble the parameter independent RB matrices A_{Nq}^{pr}, A_{Nq}^{du} and vectors $\mathbf{F}_{Nq}^{pr}$, $\mathbf{L}_{Nq}^{pr}$, $\mathbf{L}_{Nq}^{du}$. Finally, we prepare the matrices and vectors for the evaluation of the a posteriori RB error estimate. These operations have, in general, relevant computational costs being dependent on the dimension of the FE problems N_h, which is greater than that of the primal and dual RB problems, i.e. $N^{pr} << N_h$ and $N^{du} << N_h$.

In the *online* step, for any given $\boldsymbol{\mu} \in \mathcal{D}$, we assemble the parameter dependent RB matrices $A_N^{pr}(\boldsymbol{\mu})$, $A_N^{du}(\boldsymbol{\mu})$ and vectors $\mathbf{F}_N^{pr}(\boldsymbol{\mu})$, $\mathbf{L}_N^{pr}(\boldsymbol{\mu})$, $\mathbf{L}_N^{du}(\boldsymbol{\mu})$, we solve the primal and dual RB problems (40) and (45), we compute the corrected output $\widetilde{s}_N(\boldsymbol{\mu})$ and, if it is requested, we provide the a posteriori RB error estimate (65) associated with the computed output. The online computational costs can be accounted in the following manner (for more details see e.g. [11, 13, 14]):

- assembling of the RB matrices and vectors: $O\left(Q_h\left(N^{pr\,2} + N^{du\,2}\right)\right)$;
- solving the primal and dual RB linear systems[1]: $O\left(N^{pr\,3} + N^{du\,3}\right)$;

[1]The RB matrices are in general full [13, 14]; for this reason, the linear RB systems (40) and (45) can be conveniently solved by means of direct methods (see e.g. [18]) which show a computational cost of order $O(\mathcal{N}^3)$, being $\mathcal{N}$ the dimension of the system.

- computing the corrected output: $O\left(Q_h N^{pr} N^{du}\right)$;
- evaluating the a posteriori RB estimate (if requested): $O\left(Q_h^2\left(N^{pr\,2} + N^{du\,2}\right)\right)$;

let us observe that we have indicated only the orders of the dominating costs for each online step. We refer to the total online computational costs by means of the following indicator:

$$\Lambda_N = \Lambda_N(N^{pr}, N^{du}; Q_h) := N^{pr\,3} + N^{du\,3} + Q_h\left(N^{pr\,2} + N^{du\,2}\right) + Q_h N^{pr} N^{du}, \quad (75)$$

which depends on N^{pr}, N^{du} and Q_h; let us observe that Q_h depends only on the problem under consideration; this implies that, given a parametrized problem, the online computational cost depends only on the dimension of the RB problem. We chose to do not take into account in the indicator Λ_N for the costs associated with the evaluation of the a posteriori RB error estimate; this choice is due to the adaptive algorithm which we adopt and which we describe in the following Section.

Remark 3.5 *The previous offline–online decomposition is allowed by the affine decomposition hypothesis made in Sections 1.1 and 2.1 concerning with the bilinear form $A_h(\cdot,\cdot;\boldsymbol{\mu})$ and the functionals $F_h(\cdot;\boldsymbol{\mu})$ and $L(\cdot;\boldsymbol{\mu})$.*

3.4.3 Adaptive algorithm

We propose now an adaptive algorithm for the choice of the samples associated with the primal and dual samples sets $\mathcal{S}_N^{pr}$, $\mathcal{S}_N^{du}$, which we use in the offline context. The proposed strategy is based on the minimization of the computational costs (75) associated with the online step and the samples are set according to an adaptive procedure; with this aim we use the a posteriori RB error estimate (71).

The adaptive algorithm can be summarized as it follows:

1. choose a tolerance *tol* on the absolute error associated with the RB deflated output $\widetilde{s}_N(\boldsymbol{\mu})$ (58);
2. choose randomly in $\overline{\mathcal{D}}$ a sample, $\boldsymbol{\mu}_1^{pr}$, for the primal problem and another one, $\boldsymbol{\mu}_1^{du}$, for the dual one; set $N^{pr} = 1$, $N^{du} = 1$, initialize the sets $\mathcal{S}_N^{pr}$, $\mathcal{S}_N^{du}$ and build the RB spaces $\mathcal{V}_N^{pr}$, $\mathcal{V}_N^{du}$;
3. assemble the RB matrices and vectors for the primal and dual problems and the a posteriori RB output error estimate (71) (when updating the RB matrices and vectors, simply add the new entries to the old ones);
4. evaluate the primal and dual RB error bounds $\overline{\Delta}_N^{pr}(\boldsymbol{\mu})$ and $\overline{\Delta}_N^{du}(\boldsymbol{\mu})$ (see Eq.(72)), $\forall \boldsymbol{\mu} \in \overline{\mathcal{D}}$;
5. if $\max_{\boldsymbol{\mu}\in\overline{\mathcal{D}}} \overline{\Delta}_N^{pr}(\boldsymbol{\mu}) < \sqrt{tol}$ or $\max_{\boldsymbol{\mu}\in\overline{\mathcal{D}}} \overline{\Delta}_N^{du}(\boldsymbol{\mu}) < \sqrt{tol}$, jump to step 7, otherwise go to step 6 (let us observe that, in general, $N^{pr} \neq N^{du}$ and this "stopping" criterium can be fulfilled separately for the primal and dual problem);
6. set $N^{pr} = N^{pr} + 1$ and $N^{du} = N^{du} + 1$, choose the primal and dual samples as:

$$\boldsymbol{\mu}_{N^{pr}}^{pr} = \underset{\boldsymbol{\mu}\in\overline{\mathcal{D}}}{\operatorname{argmax}}\, \overline{\Delta}_{N^{pr}-1}^{pr}(\boldsymbol{\mu}), \qquad \boldsymbol{\mu}_{N^{du}}^{du} = \underset{\boldsymbol{\mu}\in\overline{\mathcal{D}}}{\operatorname{argmax}}\, \overline{\Delta}_{N^{du}-1}^{du}(\boldsymbol{\mu}), \quad (76)$$

   update the samples sets $\mathcal{S}_N^{pr}$, $\mathcal{S}_N^{du}$ and the RB spaces $\mathcal{V}_N^{pr}$, $\mathcal{V}_N^{du}$ and go back to step 3;

7. set $N^{pr}_{max} = N^{pr}$ and $N^{du}_{max} = N^{du}$ and build a matrix (table), say $D_N \in \mathbb{R}^{N^{pr}_{max} \times N^{du}_{max}}$, whose entries are:

$$(D_N)_{i,j} := \max_{\boldsymbol{\mu} \in \overline{\mathcal{D}}} \overline{\Delta}^{pr}_i(\boldsymbol{\mu})\, \overline{\Delta}^{du}_j(\boldsymbol{\mu}) \qquad i = 1, \ldots, N^{pr}_{max}, \quad j = 1, \ldots, N^{du}_{max}; \tag{77}$$

8. set a vector of prescribed "error levels", say $E_{lev} \in \mathbb{R}^Z$, s.t. $E_{lev} = \{tol_1, tol_2, \ldots, tol_Z\}$, for some $Z \in \mathbb{N}$ and $tol_1 > tol_2 > \ldots > tol_Z$, with $tol_Z \leq tol$;

9. for each error level $\{tol_m\}_{m=1}^Z$ identify the entries i_m, j_m of the matrix D_N s.t. $(D_N)_{i_m,j_m} < E_{lev}$; among these, select the coordinates N^{pr}_m and N^{du}_m s.t.:

$$\left(N^{pr}_m, N^{du}_m\right) = \underset{i_m, j_m}{\operatorname{argmin}} \Lambda_N(i_m, j_m; Q_h) \qquad \forall m = 1, \ldots, Z, \tag{78}$$

   where Λ_N is the indicator of the online computational cost (75).

10. build a matrix (table), say E_N, with Z rows and 4 columns in order to summarize the results of the whole procedure; in the first column we report the error levels vector E_{lev}, while in the following ones the corresponding number of primal and dual RB basis N^{pr}_m, N^{du}_m and the online computational costs indicator $\Lambda_N(N^{pr}_m, N^{du}_m; Q_h)$, respectively.

Remark 3.6 *The previous adaptive algorithm allows us to avoid the computation of the a posteriori RB error estimate (71) in the online context: in fact, once time we have decided an error level, it is immediate to provide the corresponding maximum error bound and the number of basis for primal and dual RB, simply by accessing to the matrix (table) E_N. Moreover, in the offline context, we assemble the RB matrices and vectors A^{pr}_{Nq}, A^{du}_{Nq}, $\mathbf{F}^{pr}_N$, $\mathbf{L}^{pr}_N$ and $\mathbf{L}^{du}_N$ for N^{pr}_{max} and N^{du}_{max}; in the online context, as observed at step 3 of the adaptive algorithm, for given $N^{pr} < N^{pr}_{max}$ and $N^{du} < N^{du}_{max}$, the corresponding RB matrices and vectors are obtained simply by eliminating the exceeding rows and columns from the "complete" RB matrices and vectors (the online computational costs associated with these operations are negligible w.r.t. other dominating costs). If a "local" error bound $\forall \boldsymbol{\mu} \in \mathcal{D}$ it is requested, the computational costs associated with the a posteriori RB error estimate should be added to the indicator (75) (see Section 3.4.2).*

Remark 3.7 *As anticipated in Remark 3.2, we have used the non integrated approach for the choice of the sets $\mathcal{S}^{pr}_N$ and $\mathcal{S}^{du}_N$. This is the consequence of the adaptive algorithm used: the crucial point it is at step 6, where the samples are chosen according to the primal and dual RB error indicators $\overline{\Delta}^{pr}_N(\boldsymbol{\mu})$ and $\overline{\Delta}^{du}_N(\boldsymbol{\mu})$. In fact, even if the primal and dual problems assume the same behavior, they can show very different solutions depending also on the functionals $F_h(\cdot; \boldsymbol{\mu})$ and $L(\cdot; \boldsymbol{\mu})$. For this reason it is evident that the samples for these problems can, and should, be different. Moreover, the adaptive algorithm adopted allows to fit the samples as best as possible, both for the primal and dual problem, even if the ultimate goal consists in computing the output functional.*

4 Combining the Finite Element and Reduced Basis Approximations

In the Sections 2 and 3 we have discussed the FE and RB methods for the numerical solution of the parametrized problem of Section 1.1. However, these approaches should not be seen as separate for the solution of our problem, but rather as complementary.

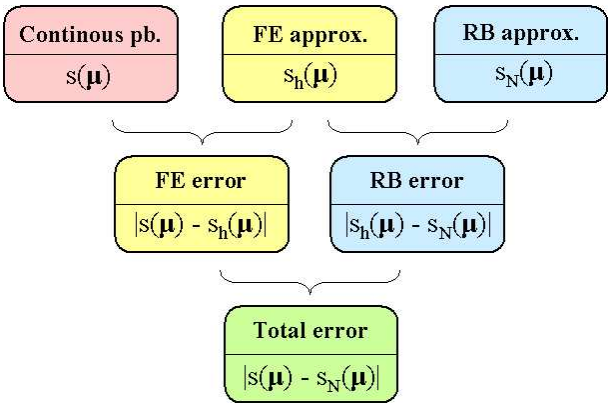

Figure 1: Scheme for numerical solution of the parameterized problem: total, FE and RB errors.

Let us recall that our continuous problem is hyperbolic as shown in Section 1.1. For the numerical approximation of this problem we have considered the FE method with stabilization; with this aim, we have provided the stabilized problem in Section 2.1 by introducing the stabilized bilinear form $A_h(\cdot,\cdot;\boldsymbol{\mu})$ and functional $F_h(\cdot;\boldsymbol{\mu})$. Let us observe that at this step, we have the following error on the output:

$$|s(\boldsymbol{\mu}) - s_h(\boldsymbol{\mu})| \qquad \text{with } \boldsymbol{\mu} \in \mathcal{D}, \tag{79}$$

where $s(\boldsymbol{\mu})$ and $s_h(\boldsymbol{\mu})$ are defined in Eq.s (5) and (17) (i.e. $\forall \boldsymbol{\mu} \in \mathcal{D}$ we solve a computational expensive FE problem). As shown by the a priori error estimate (32), the error $|s(\boldsymbol{\mu}) - s_h(\boldsymbol{\mu})| \to 0$, as $h \to 0$, $\forall \boldsymbol{\mu} \in \mathcal{D}$.
The RB method is based on the FE approximations, which are used to set the RB basis; with this aim, the stabilized Galerkin problem is used in order to define the RB method in Section 3. For this reason the RB error on the output is evaluated w.r.t. the output corresponding to the FE approximation for a given parameter $\boldsymbol{\mu} \in \mathcal{D}$, i.e.:

$$|s_h(\boldsymbol{\mu}) - s_N(\boldsymbol{\mu})| \qquad \text{with } \boldsymbol{\mu} \in \mathcal{D}, \tag{80}$$

being $s_N(\boldsymbol{\mu})$ defined in Eq.(41). The a priori RB error estimate (55) shows that the error $|s_h(\boldsymbol{\mu}) - s_N(\boldsymbol{\mu})| \to 0$, as N increases ($N \to \infty$), where N indicates generically the size of the primal and dual RB problems.
The total error on the output is composed by two terms, given form Eq.s (79) and (80):

$$|s(\boldsymbol{\mu}) - s_N(\boldsymbol{\mu})| \leq |s(\boldsymbol{\mu}) - s_h(\boldsymbol{\mu})| + |s_h(\boldsymbol{\mu}) - s_N(\boldsymbol{\mu})| \qquad \text{with } \boldsymbol{\mu} \in \mathcal{D}; \tag{81}$$

in Fig.1 the previous issues are outlined by means of a block diagram. However, even if $N \to \infty$ the total error reduces, due to the reduction of the RB part of the error, this is not the case for $h \to 0$. In fact, by referring e.g. to the Problem 1(bis), if $h \to 0$, the FE error reduces according to the a priori FE error estimate (32), but, for a prescribed N, the RB error increases; this is due to the term $\Xi(\boldsymbol{\mu})$ (51) of the a priori RB estimate (55), which is of order $h^{-1/2}$. This shows that, as $h \to 0$, for a prescribed $\boldsymbol{\mu} \in \mathcal{D}$ and a fixed N, the RB error could increase; in other words, if the stabilized problem tends to assume an hyperbolic nature (for $h \to 0$), the "complexity" of the RB problem enhances, i.e. the number of RB basis should increase in order to obtain a prescribed accuracy on the RB error.
For further examples about the RB method for hyperbolic problems, see [12, 25].

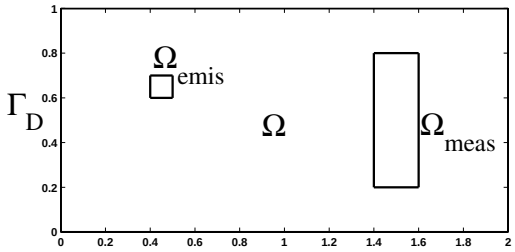

Figure 2: PB1. Domain, subdomains and Dirichlet boundary.

5 Numerical Tests

In this Section we report two numerical tests, which refer to the problems outlined in Sections 1.2 and 1.3. Both the tests are inspired by Environmental problems concerning with air pollution, for which the goal consists in evaluating the mean concentration of a pollutant in an area of interest (e.g. a city) emitted by a source (e.g. an industrial chimney) (see [4, 15, 17]). Such a pollutant is transported by a wind field and can react in air; diffusion processes are considered negligible.

5.1 Problem 1: physical parametrization

In this Section we consider the Problem 1 outlined in Section 1.2.
By referring to the problem (8), we consider the domain Ω reported in Fig.2, where we have defined two internal subdomains Ω_{emis} and Ω_{meas}. We assume $\mu \in \mathcal{D} = [1, 10^3]$, $\mathbf{V} = \hat{\mathbf{x}}$, $g = \chi_{emis}(\mathbf{x})$ and $\delta = 1/|\Omega_{meas}|\ \chi_{meas}(\mathbf{x})$, where $\chi_{emis}(\mathbf{x})$ and $\chi_{meas}(\mathbf{x})$ are the characteristic functions of the subdomains Ω_{emis} and Ω_{meas}, respectively; $|\Omega_{meas}|$ is the area of Ω_{meas}. It follows that $\Gamma_D = \{\mathbf{x} = (\mathrm{x}, \mathrm{y}) \in \partial\Omega\ :\ \mathrm{x} = 0\}$, as reported in Fig.2. This problem admits an affine decomposition on the bilinear form and functionals that define the weak problem; by referring to Section 2.1, we have $Q_h = 2$, $Q_h^F = 1$ and $Q^L = 1$ (see Eq.s (18) and (7)). In order to evaluate the norm $|||\cdot|||$, which depends on μ as reported in Section 3.4.1, we choose $\overline{\mu} = 1$; for the sake of simplicity we indicate $|||\cdot|||_{\overline{\mu}}$ simply by $|||\cdot|||$.
A quasi-uniform mesh with 7556 triangles ($h = 0.0265$) is used to solve the FE problem. Moreover, we choose the constants (15) as $\varepsilon_h = c_\varepsilon \mu h^{3/2}$ and $\delta_h = c_\delta h/\mu$, with $c_\varepsilon = 5 \cdot 10^{-2}$ and $c_\delta = 5 \cdot 10^{-2}$, which allows to contain the under and over–shooting of the FE solution $\forall \mu \in \mathcal{D}$. In Fig.3 we report the FE solutions of the primal problem for the choices $\mu = 1$ (left) and $\mu = 10^3$ (right); the corresponding FE dual solutions show similar behaviors even if the solutions arise from Ω_{meas} and the flow direction is opposite to that of the primal one.

We solve now the parametrized problem by means of the RB method outlined in Section 3 and we provide some results concerning with the a priori and a posteriori RB error estimates. We report in Fig.4 the output $s_N(\mu)$ vs $\mu \in \mathcal{D}$ computed by means of the RB method, with a number of basis "sufficiently" large s.t. $s_N(\mu)$ is a good approximation of $s_h(\mu)\ \forall \mu \in \mathcal{D}$.
In Fig.5(left) we compare the a priori RB primal error estimate (50) with the true RB error on the primal solution $|||e_N^{pr}(\mu)|||$ for different values of $\mu \in \mathcal{D}$, being $N^{pr} = 4$ with $\mathcal{S}_N^{pr} = \{1.00,\ 1.52,\ 3.06,\ 93.29\}$. In similar way, in Fig.5(right) the a priori RB error estimate for the output (55) is compared with the true output error $|s_h(\mu) -$

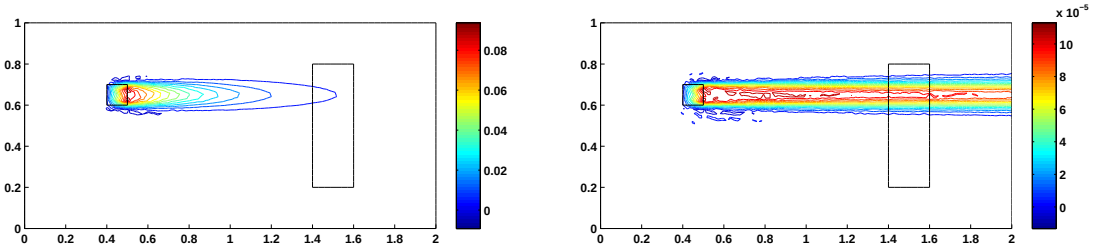

Figure 3: PB1. Primal FE solutions for $\mu = 1$ (left) and $\mu = 10^3$ (right).

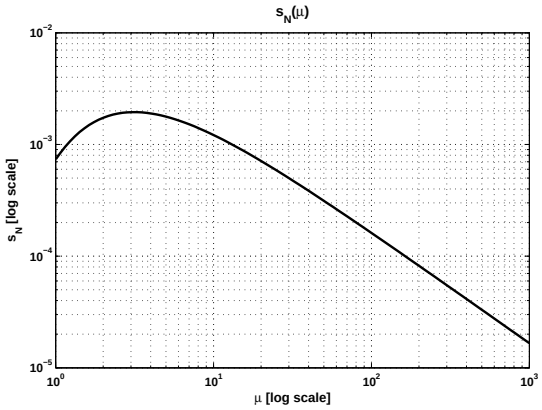

Figure 4: PB1. Output $s_N(\mu)$ vs $\mu \in \mathcal{D}$; logarithmic scale on both axis.

$s_N(\mu)|$ for $\mu \in \mathcal{D}$; in this case $N^{pr} = N^{du} = 4$, with the set $\mathcal{S}_N^{pr}$ chosen as previously mentioned and $\mathcal{S}_N^{du} = \{1.00,\ 1.42,\ 2.48,\ 9.33\}$. In order to highlight the effect of the FE mesh on $\Xi(\mu)$ (52), we compare three quasi–uniform meshes with 2680, 7556 and 17016 triangles; for example, for the previous meshes and $\mu = 10^2$, we have $\Xi(\mu) \simeq 205, 280, 325$ respectively. In general, as h decreases (i.e. the FE solution "improves"), the parametrized constant $\Xi(\mu)$ increases for any fixed values of $\mu \in \mathcal{D}$, thus affecting the sharpness property of the a priori RB estimates (50), (54) and (55).
We deals now with the a posteriori RB error estimate (65) (and (71)) which we use in the adaptive algorithm of Section 3.4.3 for the choice of the RB samples and basis. Firstly, we need to evaluate the parametrized inf–sup stability constant $\beta(\mu)$ (62); with this aim, we use the numerical procedure outlined in Section 3.4.1 (Eq.s (69) and (70)). Being $\mathcal{D} \subset \mathbb{R}$, we adopt for $\{\Pi_m(\mu)\}_{m=1}^K$ a polinomial approximation in the least–squares sense of degree 3 obtained by means of the logarithmic–equally spaced pairs $(\mu_m, \bar{\beta}(\mu_m))$, $m = 1, \ldots, K$ with $K = 9$. In Fig.6 we report the a posteriori RB error estimate for the output (65), which we evaluate by means of Eq.(71), and the true error for $N^{pr} = N^{du} = 4$; the samples sets $\mathcal{S}_N^{pr}$ and $\mathcal{S}_N^{du}$ are the same chosen for the a priori RB error estimates of Fig.s 5(left) and (right).
The a posteriori RB error estimate (71) is used in the adaptive algorithm introduced in Section 3.4.3 for the choice of $\mathcal{S}_N^{pr}$ and $\mathcal{S}_N^{du}$. The results of the adaptive algorithm

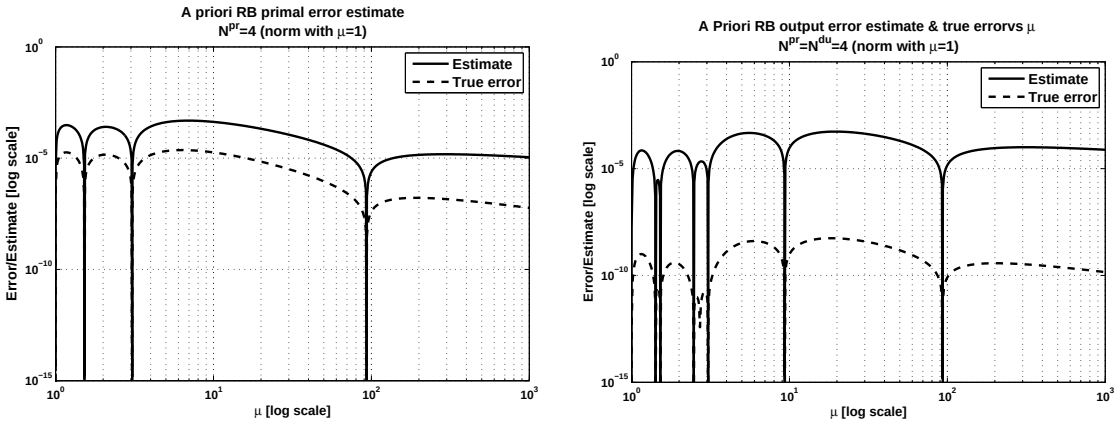

Figure 5: PB1. A priori RB error estimates (continuous) and true RB errors (dashed) vs $\mu \in \mathcal{D}$: primal RB error with $N^{pr} = 4$ (left) and output RB error with $N^{pr} = N^{du} = 4$ (right); logarithmic scales on both axis.

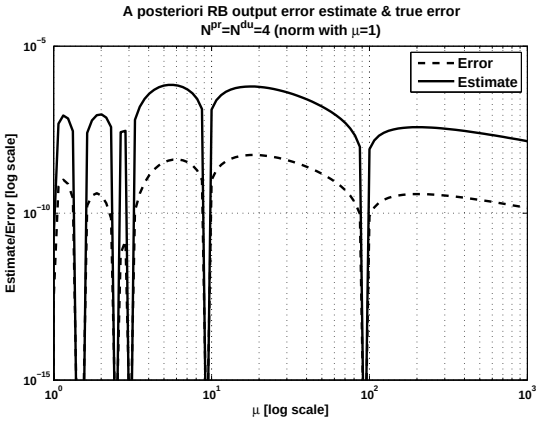

Figure 6: PB1. A posteriori RB error estimate for the output (71) with $N^{pr} = N^{du} = 4$ (continuous) and true error (dashed) vs $\mu \in \mathcal{D}$; logarithmic scales on both axis.

are summarized in Table 1 by means of the matrix (table) E_N defined at point 10 of Section 3.4.3; in order to show the effectivity of the "primal–dual" RB approach we compare the results with those of an "only primal" RB approach, evidencing the savings of computational costs allowed by the former one. In Table 1 we report, for each error level E_{lev} for the output, the selected number of basis N^{pr}, N^{du} and the computational costs associated with the "primal–dual" ($\Lambda_N^{pr,du} = \Lambda_N$, see Eq.(75)) and the "only primal" (Λ_N^{pr}) RB approaches respectively; moreover, we report the ratio $\Lambda_N^{pr}/\Lambda_N^{pr,du}$ for each error level. Let us notice that in the case for which $N^{pr} > 0$ and $N^{du} = 0$, the "primal–dual" RB approach is equivalent to the "only primal" one. As we can observe from Table 1, $\Lambda_N^{pr} \geq \Lambda_N^{pr,du}$ $\forall E_{lev}$; this shows the effectiveness of the "primal–dual" RB approach w.r.t. the "only primal" one, which is more expensive even

	"primal–dual" RB			"only primal" RB		
E_{lev}	N^{pr}	N^{du}	$\Lambda_N^{pr,du}$	N^{pr}	Λ_N^{pr}	$\Lambda_N^{pr}/\Lambda_N^{pr,du}$
$1.000e+01$	1	0	$3.000e+00$	1	$3.000e+00$	1.000
$5.623e+00$	1	0	$3.000e+00$	1	$3.000e+00$	1.000
$3.162e+00$	1	0	$3.000e+00$	1	$3.000e+00$	1.000
$1.778e+00$	1	0	$3.000e+00$	1	$3.000e+00$	1.000
$1.000e+00$	1	0	$3.000e+00$	1	$3.000e+00$	1.000
$5.623e-01$	1	0	$3.000e+00$	1	$3.000e+00$	1.000
$3.162e-01$	1	0	$3.000e+00$	1	$3.000e+00$	1.000
$1.778e-01$	1	0	$3.000e+00$	1	$3.000e+00$	1.000
$1.000e-01$	1	0	$3.000e+00$	1	$3.000e+00$	1.000
$5.623e-02$	1	1	$8.000e+00$	2	$1.600e+01$	2.000
$3.162e-02$	2	0	$1.600e+01$	2	$1.600e+01$	1.000
$1.778e-02$	1	2	$2.300e+01$	3	$4.500e+01$	1.957
$1.000e-02$	2	2	$4.000e+01$	3	$4.500e+01$	1.125
$5.623e-03$	3	0	$4.500e+01$	3	$4.500e+01$	1.000
$3.162e-03$	3	0	$4.500e+01$	3	$4.500e+01$	1.000
$1.778e-03$	1	3	$5.400e+01$	4	$9.600e+01$	1.778
$1.000e-03$	2	3	$7.300e+01$	4	$9.600e+01$	1.315
$5.623e-04$	2	3	$7.300e+01$	4	$9.600e+01$	1.315
$3.162e-04$	4	0	$9.600e+01$	4	$9.600e+01$	1.000
$1.778e-04$	4	1	$1.070e+02$	5	$1.750e+02$	1.636
$1.000e-04$	4	1	$1.070e+02$	5	$1.750e+02$	1.636
$5.623e-05$	4	2	$1.280e+02$	5	$1.750e+02$	1.367
$3.162e-05$	4	3	$1.650e+02$	5	$1.750e+02$	1.061
$1.778e-05$	4	3	$1.650e+02$	6	$2.880e+02$	1.745
$1.000e-05$	4	3	$1.650e+02$	6	$2.880e+02$	1.745
$5.623e-06$	4	3	$1.650e+02$	6	$2.880e+02$	1.745
$3.162e-06$	5	2	$2.110e+02$	6	$2.880e+02$	1.365
$1.778e-06$	4	4	$2.240e+02$	6	$2.880e+02$	1.286
$1.000e-06$	4	4	$2.240e+02$	6	$2.880e+02$	1.286
$5.623e-07$	3	5	$2.500e+02$	7	$4.410e+02$	1.764
$3.162e-07$	5	4	$3.110e+02$	7	$4.410e+02$	1.418
$1.778e-07$	5	4	$3.110e+02$	7	$4.410e+02$	1.418
$1.000e-07$	5	4	$3.110e+02$	7	$4.410e+02$	1.418
$5.623e-08$	5	4	$3.110e+02$	7	$4.410e+02$	1.418
$3.162e-08$	5	4	$3.110e+02$	8	$6.400e+02$	2.058
$1.778e-08$	5	4	$3.110e+02$	8	$6.400e+02$	2.058
$1.000e-08$	5	5	$4.000e+02$	8	$6.400e+02$	1.600
$5.623e-09$	5	5	$4.000e+02$	9	$8.910e+02$	2.228
$3.162e-09$	6	4	$4.320e+02$	9	$8.910e+02$	2.062
$1.778e-09$	6	5	$5.230e+02$	9	$8.910e+02$	1.704
$1.000e-09$	6	5	$5.230e+02$	9	$8.910e+02$	1.704
$5.623e-10$	6	5	$5.230e+02$	9	$8.910e+02$	1.704
$3.162e-10$	6	5	$5.230e+02$	10	$1.200e+03$	2.294
$1.778e-10$	6	5	$5.230e+02$	10	$1.200e+03$	2.294
$1.000e-10$	6	6	$6.480e+02$	10	$1.200e+03$	1.852
$5.623e-11$	6	6	$6.480e+02$	10	$1.200e+03$	1.852
$3.162e-11$	6	6	$6.480e+02$	10	$1.200e+03$	1.852
$1.778e-11$	5	7	$6.860e+02$			
$1.000e-11$	6	7	$8.130e+02$			
$5.623e-12$	6	7	$8.130e+02$			
$3.162e-12$	6	7	$8.130e+02$			
$1.778e-12$	6	7	$8.130e+02$			
$1.000e-12$	5	8	$8.950e+02$			

Table 1: PB1. Adaptive algorithm: results of samples selection procedure and comparison between the 'primal–dual" and the "only primal" RB approach.

for this simple test problem with a single parameter μ. For example, if we require an error level $E_{lev} = 10^{-8}$ (i.e. the relative error on $s(\mu)$ is inferior to 0.1% $\forall \mu \in \mathcal{D}$, see Fig.4) the "primal–dual" RB approach selects $N^{pr} = N^{du} = 5$ w.r.t. $N^{pr} = 8$ requested by the "only primal" RB approach and it allows a saving of the online computational costs of about the 60%. We notice that even larger computational costs savings can be obtained; e.g. for $E_{lev} = 1.778 \cdot 10^{-10}$, the saving is about the 130%. Let us observe that the adaptive algorithm does not tend to select the case $N^{du} = 0$ as E_{lev} decreases;

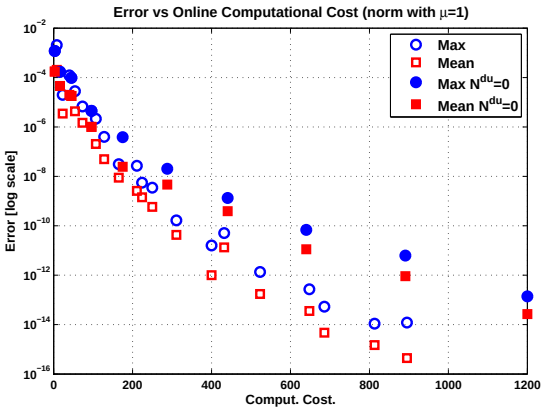

Figure 7: PB1. E_N^{max} (empty circle) and E_N^{mean} (empty square) for the "primal–dual" RB approach vs online computational costs $\Lambda_N^{pr,du}$, Λ_N^{pr}; full circles and squares refer to the indicators E_N^{max}, E_N^{mean} for the "only primal" RB approach. Error axis in logarithmic scale.

in fact, $\Lambda_N^{pr,du}$ increases if $N^{pr} \neq N^{du}$.
Finally, we compare the true RB errors for the output obtained by using the adaptive algorithm for the "primal–dual" RB approach with those of the "only primal" one; with this aim we recall the RB error indicators for the output E_N^{max} and E_N^{mean} (see Eq.(73)). In Fig.7 we report E_N^{max} and E_N^{mean} vs the online computational cost $\Lambda_N^{pr,du}$ and Λ_N^{pr} for both the "primal–dual" and "only primal" RB approaches. The plot shows that the "primal–dual" RB approach allows to minimize the online computational costs for any given error tolerance on the output; for example if we fix the tolerance error at 10^{-12} we see that $\Lambda_N^{pr,du}$ is about the half of Λ_N^{pr}. This confirms, a posteriori, the validity of the adaptive algorithm and the criterium of the "minimum online computational costs". We observe that the effectivity index indicators $\overline{\eta}_N \in [20, 700]$ for both the RB approaches, with no particular differences.

5.2 Problem 2: physical and geometrical parametrization

We consider now the Problem 2 of Section 1.3.

As anticipated in Section 1.3, we introduce the geometrical parameter, μ_g s.t. the real domain Ω_0 could be affinely mapped into a reference one Ω. In Fig.8(left) we report the real domain Ω_0, which is partitioned into 5 subdomains Ω_{0i}, s.t. $\cup_{i=1}^5 \Omega_{0i} = \Omega_0$. The geometrical parameter μ_g (with signum) measures the distance between the mid abscissa of the subdomain Ω_{03} and the coordinate $x_0 = 0$; the subdomains Ω_{01} and Ω_{05} are fixed, while Ω_{02} and Ω_{04} deform in affine manner according to the moving of Ω_{03}. All the subdomains Ω_{0i} can be mapped in Ω by means of affine maps in the form (11); the reference domain $\Omega = \cup_{i=1}^5 \Omega_i$ is reported in Fig.8(right). We remark that the subdomains Ω_{emis} and Ω_{meas} move fixed with the subdomains Ω_{03} and Ω_{05} respectively; the Dirichlet boundary corresponds to the upper boundary of Ω.
The parameter vector $\boldsymbol{\mu} = (\mu_g, \mu_p)$ is taken in the parameter domain $\mathcal{D} = [\mu_g^{min}, \mu_g^{max}] \times [\mu_p^{min}, \mu_p^{max}]$, where we choose $\mu_g^{min} = -3/8$, $\mu_g^{max} = 3/8$, $\mu_p^{min} = 1$ and $\mu_p^{max} = 10^3$.

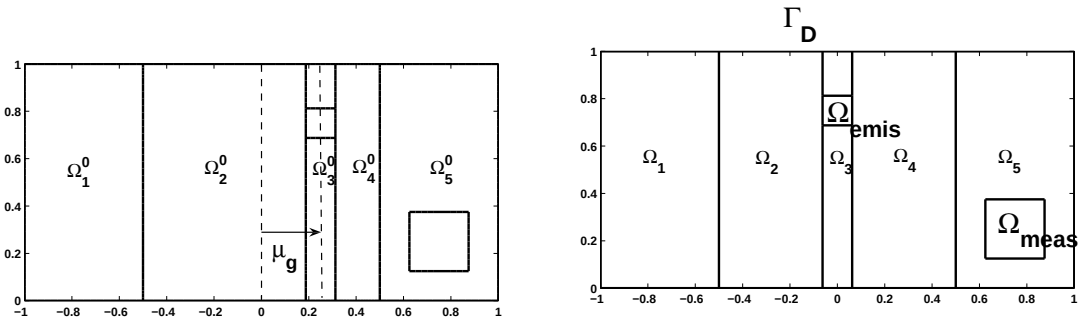

Figure 8: PB2. Real Ω_0 (left) and reference Ω (right) domains; geometrical parameter and Dirichlet boundary.

We observe that the choices made for μ_g^{min} and μ_g^{max} do not allow the degeneration of the subdomains Ω_{02} and Ω_{04}. By recalling the notation of Sections 1.3 and 5.1, we choose $\mathbf{V}_0 = \mathrm{x}_0\hat{\mathbf{x}} - \mathrm{y}_0\hat{\mathbf{y}}$, $g_0 = \chi_{meas}(\mathbf{x}_0)$ and $\delta_0 = 1/|\Omega_{meas}|\ \chi_{meas}(\mathbf{x}_0)$. By considering the data reported on the reference domain (see Eq.(12)), we obtain the problem in the general weak form (2). It is simple to show that, for the problem under consideration, the hypothesis on the data requested in Section 1.1 are satisfied; in particular the property $\nabla \cdot \mathbf{b}(\boldsymbol{\mu}) = 0\ \forall \boldsymbol{\mu} \in \mathcal{D}$ holds. The weak problem admits an affine decomposition for which we have $Q_h = 16$, $Q_h^F = 2$ and $Q^L = 1$ (see Eq.s (15) and (7)). As reported in Section 3.4.1, for the evaluation of the norm $|||\cdot|||$ we choose $\overline{\boldsymbol{\mu}} = (\overline{\mu}_g, \overline{\mu}_p) = (0, 1)$
For the FE solution of the problem we choose a quasi–uniform mesh for the reference domain Ω with 7504 triangles and the constants (15) as $\varepsilon_h(h, \mu_p) = c_\varepsilon \mu_p h^{3/2}$ and $\delta_h = c_\delta h/\mu_p$ with $c_\varepsilon = 2 \cdot 10^{-1}$ and $c_\delta = 2 \cdot 10^{-1}$. In Fig. 9 we report the primal FE solutions, mapped from Ω into Ω_0, for different choices of $\boldsymbol{\mu}$. We observe that, if $\mu_g = 0\ \forall \mu_p \in [\mu_p^{min}, \mu_p^{max}]$, $\Omega_0 \equiv \Omega$. As shown, the primal solution strongly depends on the values assumed by the geometrical parameter μ_p and not only by the physical one μ_p. On the contrary, for this particular problem, the behavior of the dual solution in the real domain Ω_0 is not influenced by the geometrical parameter, being the "dual source" subdomain Ω_{meas} fixed. However, this is not true in the reference domain Ω, being the weak form of the stabilized dual problem (21) depending on μ_g.

We solve the parametrized problem by means of the RB method and we discuss the results about the adaptive algorithm and the a posteriori RB estimate.
In Fig.10 we report the output $s_N(\boldsymbol{\mu})$ vs $\boldsymbol{\mu} \in \mathcal{D}$, where we notice that $s_N(\boldsymbol{\mu})$ is maximum for about $\boldsymbol{\mu} = (0.28, 3.0)$; we recall that the RB output $s_N(\boldsymbol{\mu})$ is a good approximation of $s_h(\boldsymbol{\mu})$ if N is "sufficiently" large.
We deals now with the a posteriori RB error estimate for the output (65) (and (71)) and the adaptive algorithm for the samples selection (see Section 3.4.3). In order to use the estimate (71), we need to evaluate the inf–sup constant; with this aim, we adopt the procedure of Section 3.4.1 obtaining the parametrized constant $\widetilde{\beta}(\boldsymbol{\mu})$ (70), with $K = 195$.
The a posteriori RB error estimate (71) is used in the adaptive algorithm in order to define the sets $\mathcal{S}_N^{pr}$ and $\mathcal{S}_N^{du}$. The results are reported in Table 2 by using the matrix E_N defined at point 10 of Section 3.4.3; the same notation of Table 1 is used for Table 2. Once time, we observe that $\Lambda_N^{pr} \geq \Lambda_N^{pr,du}\ \forall E_{lev}$. E.g., if we fix $E_{lev} = 10^{-5}$, we see

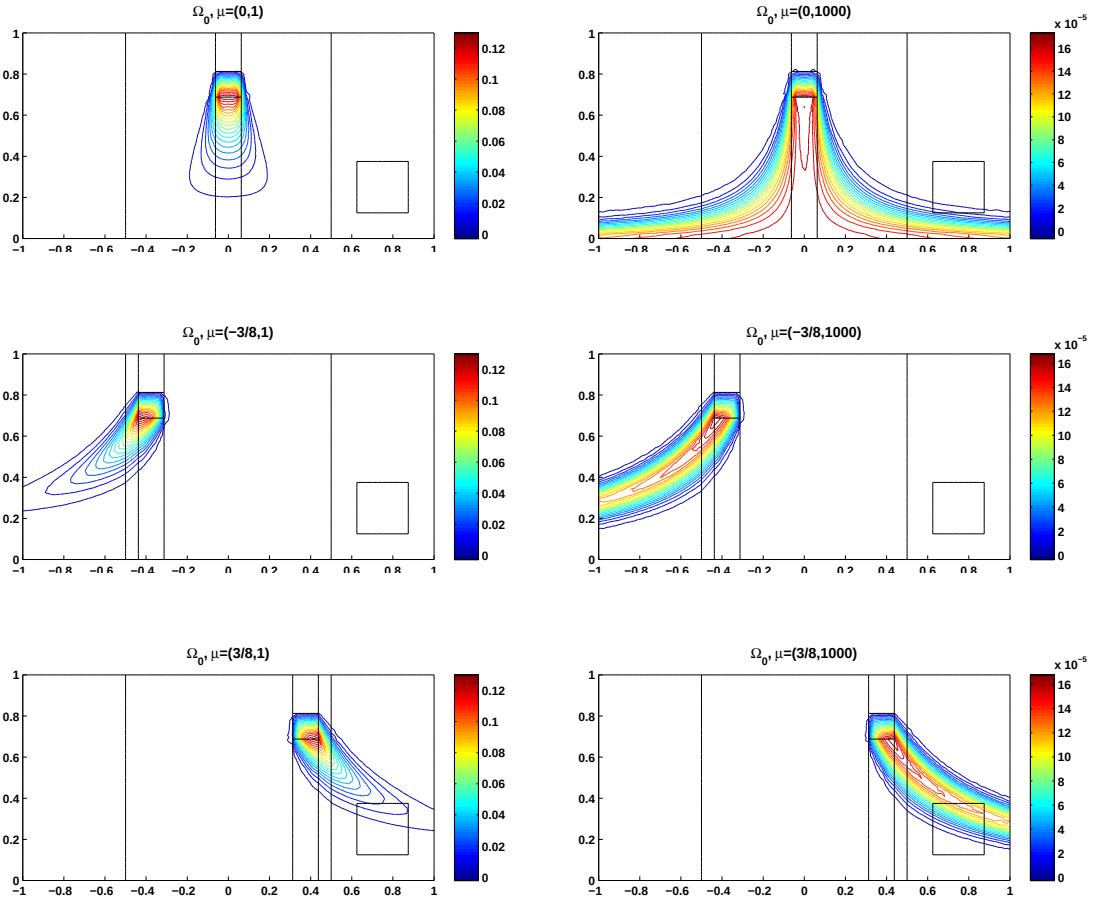

Figure 9: PB2. Primal FE solutions in the real domain Ω_0 for $\boldsymbol{\mu} = (0, 1)$ (top–left), $\boldsymbol{\mu} = (0, 10^3)$ (top–right), $\boldsymbol{\mu} = (-3/8, 1)$ (mid–left), $\boldsymbol{\mu} = (-3/8, 10^3)$ (mid–right), $\boldsymbol{\mu} = (3/8, 1)$ (bottom–left) and $\boldsymbol{\mu} = (3/8, 10^3)$ (bottom–right).

from Table 2 that the "primal–dual" RB approach selects $N^{pr} = 27$ and $N^{du} = 41$ w.r.t. $N^{pr} = 113$ chosen by the "only primal" one; morevover, the saving of online computational cost is considerable, being of about 11 times inferior. Even larger savings are allowed for the problem under consideration: for example, if $E_{lev} = 5.623 \cdot 10^{-4}$ we have $\Lambda_N^{pr}/\Lambda_N^{pr,du} = 15.687$.
We compare the true RB errors for the output obtained on the basis of the adaptive algorithm for the "primal–dual" and the "only primal" RB approaches. In Fig.11 we report the error indicators E_N^{max} and E_N^{mean} (see Eq.(73)) vs the online computational costs $\Lambda_N^{pr,du}$ and Λ_N^{pr} for both the "primal–dual" and "only primal" RB approaches. The plot clearly shows that the "primal–dual" RB allows great savings of online computational costs for any given error tolerance on the output; for example, if we fix the tolerance error at 10^{-8} we see that $\Lambda_N^{pr,du}$ is about 8 times inferior than Λ_N^{pr}. This

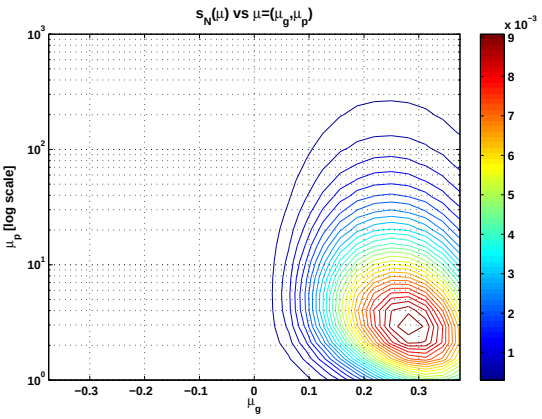

Figure 10: PB2. Contourlines of $s_N(\boldsymbol{\mu})$ vs $\boldsymbol{\mu} = (\mu_g, \mu_p) \in \mathcal{D}$; axis μ_p in logarithmic scale.

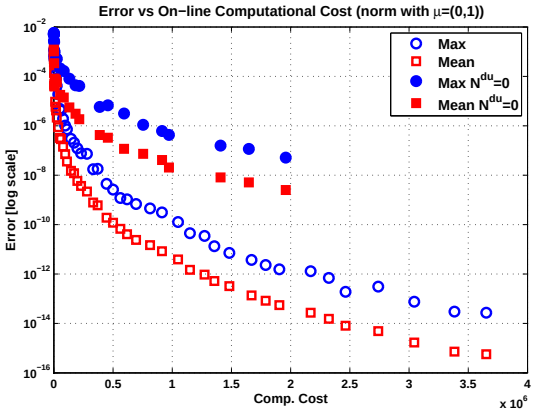

Figure 11: PB2. E_N^{max} (empty circle) and E_N^{mean} (empty square) for the "primal–dual" RB approach vs online computational costs $\Lambda_N^{pr,du}$, Λ_N^{pr}; full circles and squares refer to the indicators E_N^{max}, E_N^{mean} for the "only primal" RB approach. Error axis in logarithmic scale.

confirms the validity of the adaptive algorithm and the indications given in Table 2. Finally, we observe that the effectivity index indicator $\overline{\eta}_N \in [10, 100]$ (see Eq.(74)) for both the approaches.

	"primal–dual" RB			"only primal" RB		
E_{lev}	N^{pr}	N^{du}	$\Lambda_N^{pr,du}$	N^{pr}	Λ_N^{pr}	$\Lambda_N^{pr}/\Lambda_N^{pr,du}$
$1.000e+01$	1	0	$1.700e+01$	1	$1.700e+01$	1.000
$5.623e+00$	1	0	$1.700e+01$	1	$1.700e+01$	1.000
$3.162e+00$	1	0	$1.700e+01$	1	$1.700e+01$	1.000
$1.778e+00$	1	0	$1.700e+01$	1	$1.700e+01$	1.000
$1.000e+00$	1	0	$1.700e+01$	1	$1.700e+01$	1.000
$5.623e-01$	1	0	$1.700e+01$	1	$1.700e+01$	1.000
$3.162e-01$	2	2	$2.080e+02$	4	$3.200e+02$	1.538
$1.778e-01$	4	0	$3.200e+02$	4	$3.200e+02$	1.000
$1.000e-01$	1	5	$6.220e+02$	11	$3.267e+03$	5.252
$5.623e-02$	1	6	$9.050e+02$	15	$6.975e+03$	7.707
$3.162e-02$	7	5	$2.212e+03$	22	$1.839e+04$	8.315
$1.778e-02$	7	7	$3.038e+03$	25	$2.562e+04$	8.435
$1.000e-02$	5	11	$4.672e+03$	33	$5.336e+04$	11.421
$5.623e-03$	7	12	$6.503e+03$	39	$8.366e+04$	12.864
$3.162e-03$	5	17	$1.142e+04$	46	$1.312e+05$	11.486
$1.778e-03$	10	17	$1.486e+04$	52	$1.839e+05$	12.376
$1.000e-03$	14	17	$1.922e+04$	55	$2.148e+05$	11.172
$5.623e-04$	14	20	$2.476e+04$	68	$3.884e+05$	15.687
$3.162e-04$	20	21	$3.744e+04$	72	$4.562e+05$	12.186
$1.778e-04$	14	29	$5.022e+04$	79	$5.929e+05$	11.806
$1.000e-04$	21	28	$6.022e+04$	86	$7.544e+05$	12.527
$5.623e-05$	20	33	$7.832e+04$	92	$9.141e+05$	11.671
$3.162e-05$	26	33	$9.548e+04$	94	$9.720e+05$	10.180
$1.778e-05$	29	34	$1.114e+05$	107	$1.408e+06$	12.639
$1.000e-05$	27	41	$1.449e+05$	113	$1.647e+06$	11.370
$5.623e-06$	26	45	$1.706e+05$	120	$1.958e+06$	11.477
$3.162e-06$	29	47	$1.988e+05$			
$1.778e-06$	30	50	$2.304e+05$			
$1.000e-06$	39	50	$2.799e+05$			
$5.623e-07$	49	47	$3.321e+05$			
$3.162e-07$	50	50	$3.700e+05$			
$1.778e-07$	44	61	$4.456e+05$			
$1.000e-07$	50	61	$5.003e+05$			
$5.623e-08$	47	67	$5.621e+05$			
$3.162e-08$	54	66	$6.183e+05$			
$1.778e-08$	60	66	$6.942e+05$			
$1.000e-08$	55	76	$8.130e+05$			
$5.623e-09$	50	83	$9.134e+05$			
$3.162e-09$	61	83	$1.050e+06$			
$1.778e-09$	57	89	$1.150e+06$			
$1.000e-09$	74	83	$1.273e+06$			
$5.623e-10$	73	87	$1.356e+06$			
$3.162e-10$	79	87	$1.482e+06$			
$1.778e-10$	77	95	$1.670e+06$			
$1.000e-10$	78	98	$1.789e+06$			
$5.623e-11$	77	102	$1.905e+06$			
$3.162e-11$	85	104	$2.169e+06$			
$1.778e-11$	93	102	$2.322e+06$			
$1.000e-11$	94	105	$2.464e+06$			
$5.623e-12$	107	100	$2.739e+06$			
$3.162e-12$	110	105	$3.043e+06$			
$1.778e-12$	116	107	$3.383e+06$			
$1.000e-12$	126	101	$3.652e+06$			

Table 2: PB2. Adaptive algorithm: results of samples selection procedure and comparison between the 'primal–dual" and the "only primal" RB approach.

Conclusions

In this work we have considered the RB method for the approximation of parametrized advection–reaction PDEs. We have generated the basis by means of the FE method applied to the stabilized version of the weak problem. For the RB method, in the "primal–dual" formulation, we have provided both a priori and a posteriori RB error estimates. We have shown that the RB "complexity" increases as the FE mesh size

reduces, thus requiring a larger number of basis in order to satisfy a prescribed tolerance on the error. An adaptive algorithm for the selection of the sample sets, based on a criterium of minimization of the online computational costs, has been proposed. We have proved, by means of numerical tests, the effectiveness of this algorithm and the savings of computational costs allowed by the "primal–dual" RB approach w.r.t. those of the "only primal" one. The numerical tests also show that if the FE approximation is stable, then so it is the RB one.

Acknowledgements

Many thanks to Prof. A.T. Patera for having introduced me to the world of the Reduced Basis method and for having welcomed me in his group at M.I.T., Mech. Eng. Dept., Microfluids Lab. Special thanks to Dr. G. Rozza for the support, helpful discussions and friendship. Thanks to Dr. G.S.H. Pau, Dr. S. Sen and D. Blanchard for the suggestions, ideas and friendly help. Many thanks to Prof. A. Quarteroni for the interst, research guidelines and for having encouraged this initiative.
The author acknowledges the financial support provided through the "Progetto Roberto Rocca", M.I.T.–Politecnico di Milano collaboration. Many thanks to Dr. S. Sferza and Prof. F. Gazzola for the kind help.

References

[1] I. Babŭska. Error–bounds for finite element method. *Numer. Math.* 16:322–333, 1971.

[2] É. Cancès, C. Le Bris, Y. Maday, N.C. Nguyen, A.T. Patera, G.S.H. Pau. Feasibility and competitiveness of a reduced basis approach for rapid electronic structure calculations in quantum chemistry. *Centre de Recherches Mathématiques, CRM Proceedings and Lecture Notes*, 2007. To appear.

[3] L. Dedè. Advanced numerical methods for the solution of optimal control problems governed by PDEs with Environmental applications. PhD Thesis, Politecnico di Milano, 2008. In progress.

[4] L. Dedè, A. Quarteroni. Optimal control and numerical adaptivity for advection–diffusion equations. *Math. Model. Numer. Anal.* 39(5):1019–1040, 2005.

[5] M.A. Grepl. Reduced–basis approximations and a posteriori error estimation for parabolic partial differential equations, PhD Thesis, MIT, 2005. `http://augustine.mit.edu/`

[6] M.A. Grepl, A.T. Patera. A posteriori error bounds for reduced–basis approximations of parametrized parabolic partial differential equations. *Math. Model. Numer. Anal.* 39(1):157–181, 2005.

[7] C. Johnson. *Numerical Solution of Partial Differential Equations by the Finite Element Method*. Cambridge University Press, Cambridge, 1987.

[8] C. Johnson, A.H. Schatz, L.B. Wahlbin. Crosswind smear and pointwise errors in streamline diffusion finite element methods. *Math. Comp.* 49(179):25–38, 1987.

[9] J.L. Lions, E. Magenes. *Non–homogeneous Boundary Value Problems and Applications*, Vol.I. Springer–Verlag, New York and Heidelberg, 1972.

[10] A.E. Løvgren, Y. Maday, E. Rønquist. A reduced basis element method for the steady Stokes problem. *Math. Model. Numer. Anal.* 40(3):529–552, 2006.

[11] N.C. Nguyen, K. Veroy, A.T. Patera. Certified real–time solution of parametrized partial differential equations. In *Handbook of Materials Modeling*, 1523–1558, S. Yip (ed.), Springer, 2005.

[12] A.T. Patera, E. Rønquist. Reduced basis approximations and a posteriori error estimation for a Boltzmann model. *Comput. Methods Appl. Mech. Engrg.* 196(29–30):2925–2942, 2007.

[13] A.T. Patera, G. Rozza. *Reduced Basis Approximation and A Posteriori Error Estimation for Parametrized Partial Differential Equations*. Version 1.0, Copyright MIT 2006–2007. To appear in (tentative rubric) MIT Pappalardo Graduate Monographs in Mechanical Engineering. `http://augustine.mit.edu/`

[14] C. Prud'homme, D. Rovas, K. Veroy, Y. Maday, A.T. Patera, G. Turinici. Reliable real–time solution of parametrized partial differential equations: reduced–basis output bound methods. *J. Fluids Eng.* 124(1):70–80, 2002.

[15] A. Quarteroni, A. Quaini, G. Rozza. Reduced basis methods for advection–diffusion optimal control problems. In *Advances in Numerical Mathematics*, 193–216, W. Fitzgibbon, R. Hoppe, J. Periaux, O. Pironneau and Y. Vassilevski (ed.s), Moscow, Russian Acedemy of Science and Houston, University of Houston, 2006.

[16] A. Quarteroni, G. Rozza. Numerical solutions of parametrized Navier–Stokes equations by reduced basis method. *Numer. Methods Partial Differential Eq.s* 23(4):923–948, 2007.

[17] A. Quarteroni, G. Rozza, L. Dedè, A. Quaini. Numerical approximation of a control problem for advection-diffusion processes. In *System modeling and optimization*, 261–273, *IFIP Int. Fed. Inf. Process.* 199, Springer, New York, 2006.

[18] A. Quarteroni, R. Sacco, F. Saleri. *Numerical Mathematics.* Springer–Verlag, Berlin, 2007.

[19] A. Quarteroni, A. Valli. *Numerical Approximation of Partial Differential Equations.* Springer, Berlin and Heidelberg, 1994.

[20] G. Rozza. Optimal flow control and reduced basis techniques in shape design with applications in haemodynamics. PhD Thesis, EPFL, 2005. `http://library.epfl.ch/theses/`

[21] G. Rozza. Reduced–basis methods for elliptic equations in sub–domains with a posteriori error bounds and adaptivity. *Appl. Numer. Math.* 55(4):403–424, 2005.

[22] G. Rozza. Reduced basis methods for Stokes equations in domains with non affine parameter dependence. *Comput. Vis. Sci.*, 2007. To appear.
Available on line `http://springerlink.metapress.com/content/100525/`

[23] G. Rozza, K. Veroy. On the stability of the reduced basis method for Stokes equations in parametrized domains. *Comput. Methods Appl. Mech. Engrg.* 196(7):1244-1260, 2007

[24] S. Sen, K. Veroy, D.B.P. Huynh, S. Deparis, N.C. Nguyen, A.T. Patera. "Natural norm" a posteriori error estimators for reduced basis approximations. *J. Comput. Phys.* 217(1):37–62, 2006.

[25] A. Tan Yong Kwang. Reduced basis method for 2*nd* order wave equation: application to one–dimension seismic problem. Master Thesis, Singapore–MIT Alliance, National University of Singapore, 2006. `http://augustine.mit.edu/`

[26] K. Veroy. Reduced–basis methods applied to problems in elasticity: analysis and applications. PhD Thesis, MIT, 2003. `http://augustine.mit.edu/`

[27] K. Veroy, A.T. Patera. Certified real–time solution of the parametrized steady incompressible Navier–Stokes equations: rigorous reduced–basis a posteriori error bounds. *Internat. J. Numer. Methods Fluids* 47:773–788, 2005

[28] G. Zhou. How accurate is the streamline diffusion finite element method? *Math. Comp.* 66(217):31–44, 1997.